# New Orleans and Hurricane Katrina. II: The Central Region and the Lower Ninth Ward

R. B. Seed, M.ASCE;[1]; R. G. Bea, F.ASCE[2]; A. Athanasopoulos-Zekkos, S.M.ASCE[3]; G. P. Boutwell, F.ASCE[4]; J. D. Bray, F.ASCE[5]; C. Cheung, M.ASCE[6]; D. Cobos-Roa[7]; L. Ehrensing, M.ASCE[8]; L. F. Harder Jr., M.ASCE[9]; J. M. Pestana, M.ASCE[10]; M. F. Riemer, M.ASCE[11]; J. D. Rogers, M.ASCE[12]; R. Storesund, M.ASCE[13]; X. Vera-Grunauer, M.ASCE[14]; and J. Wartman, M.ASCE[15]

**Abstract:** The failure of the New Orleans regional flood protection systems, and the resultant catastrophic flooding of much of New Orleans during Hurricane Katrina, represents the most costly failure of an engineered system in U.S. history. This paper presents an overview of the principal events that unfolded in the central portion of the New Orleans metropolitan region during this hurricane, and addresses the levee failures and breaches that occurred along the east–west trending section of the shared Gulf Intracoastal Waterway/Mississippi River Gulf Outlet channel, and along the Inner Harbor Navigation Channel, that affected the New Orleans East, the St. Bernard Parish, and the Lower Ninth Ward protected basins. The emphasis in this paper is on geotechnical lessons, and also broader lessons with regard to the design, implementation, operation, and maintenance of major flood protection systems. Significant lessons learned here in the central region include: (1) the need for regional-scale flood protection systems to perform as systems, with the various components meshing well together in a mutually complementary manner; (2) the importance of considering all potential failure modes in the engineering design and evaluation of these complex systems; and (3) the problems inherent in the construction of major regional systems over extended periods of multiple decades. These are important lessons, as they are applicable to other regional flood protection systems in other areas of the United States, and throughout much of the world.

**DOI:** 10.1061/(ASCE)1090-0241(2008)134:5(718)

**CE Database subject headings:** Louisiana; Hurricanes; Floods; Failures.

## Introduction

This paper is the second of a series of companion papers that together present a number of the principal results of an investigation of the performance of the New Orleans regional flood protection systems during and after Hurricane Katrina, which struck the New Orleans region on August 29, 2005. A more complete report on these studies by the Independent Levee Investigation Team (ILIT) can be found in ILIT (2006) and Seed et al. (private communication, 2008). This paper addresses events that unfolded in the central part of the devastated region, producing levee failures and breaches along the east–west trending combined Mississippi River Gulf Outlet (MRGO)/Gulf Intracoastal Waterway (GIWW) channel and along the Inner Harbor Navigation Channel (IHNC).

New Orleans is situated mainly between Lake Pontchartrain to the north, the Mississippi River to the south, and Lake Borgne, immediately to the east. Fig. 1 shows the three main protected "polders" or levee-protected basins of the New Orleans metropolitan area: (1) the New Orleans East protected basin; (2) the St.

[1]Professor of Civil and Environmental Engineering, Univ. of California, Berkeley, CA.
[2]Professor of Civil and Environmental Engineering, Univ. of California, Berkeley, CA.
[3]Doctoral Candidate, Dept. of Civil and Environmental Engineering, Univ. of California, Berkeley, CA.
[4]Senior Consultant, Ardaman & Associates, Inc., Baton Rouge and New Orleans, LA.
[5]Professor of Civil and Environmental Engineering, Univ. of California, Berkeley, CA.
[6]Engineer I, PB Americas Inc., San Francisco, CA.
[7]Engineer, URS Corp., Oakland, CA.
[8]Engineer, URS Corp., Oakland, CA.
[9]Senior Water Resources Technical Advisor, HDR Inc., Folsom, CA.
[10]Professor of Civil and Environmental Engineering, Univ. of California, Berkeley, CA.
[11]Professor of Civil and Environmental Engineering, Univ. of California, Berkeley, CA.
[12]Hasselmann Professor of Geological Engineering, Missouri Univ. of Science and Technology, Rolla, MO.
[13]Consulting Engineer, Rune Storesund, Albany, CA.
[14]Senior Project Engineer, CVA Consulting Group, Guayaquil, Ecuador.
[15]Associate Professor of Civil, Architectural and Environmental Engineering, Drexel Univ., PA.

Note. Discussion open until October 1, 2008. Separate discussions must be submitted for individual papers. To extend the closing date by one month, a written request must be filed with the ASCE Managing Editor. The manuscript for this paper was submitted for review and possible publication on April 23, 2007; approved on January 25, 2008. This paper is part of the ***Journal of Geotechnical and Geoenvironmental Engineering***, Vol. 134, No. 5, May 1, 2008. ©ASCE, ISSN 1090-0241/2008/5-718–739/$25.00.

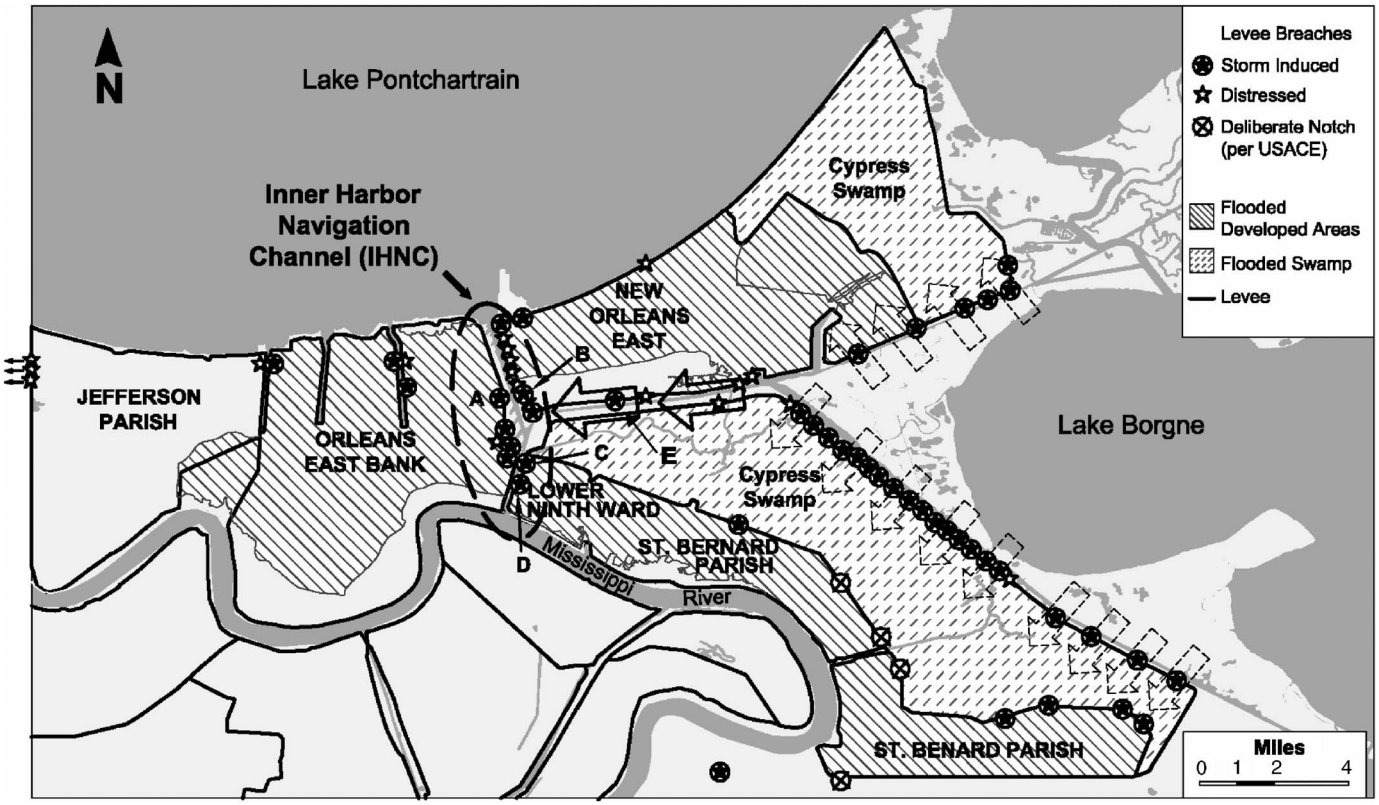


**Fig. 1.** Map schematically illustrating the lateral flow from Lake Borgne to the IHNC, and showing the locations of breaches and partial breaches in the IHNC region and vicinity

Bernard and Lower Ninth Ward protected basin; and (3) the main ("downtown") Orleans East Bank metropolitan basin. Fig. 1 also shows the locations of levee failures (breaches), partial breaches, and incipient failures that occurred in this region. The closed stars within circles in Fig. 1 show the locations of levee breaches and/or floodwall failures, and the open stars without circles show the locations of partial breaches and/or significant levee distress. The ×'s in Fig. 1 show the locations of deliberate "notches" in the levees that were created after the storm had passed to facilitate outward drainage of floodwaters from within the flooded basins.

## Phase Three: Storm Surge and Failures in the Central Region

The catastrophic flooding produced by Hurricane Katrina unfolded progressively in four main phases as the storm advanced. The first two phases were discussed in the preceding companion paper in this series (Seed et al. 2008a). These were: (1) the inundation of Plaquemines Parish (on the lower reaches of the Mississippi River south of St. Bernard Parish, just to the south of the map of Fig. 1); and then (2) the extensive erosional failures along the east flank of the regional flood protection system as the storm surge first inflated the waters of Lake Borgne and then the storm surge and wind-driven waves passed both over and through the Lake Borgne frontage levees (as indicated by dashed arrows in Fig. 1).

This paper discusses the third phase of the storm as the swollen waters of Lake Borgne were pushed westward along the east–west trending GIWW/MRGO channel. This combined channel forms a "T" intersection at its western end where it meets the north–south trending Inner Harbor Navigation Channel (IHNC). The south end of the IHNC is closed off by a navigational lock just to the south of Location "D" in Fig. 1 (providing controlled access to the main Mississippi River), so the storm surge flow from Lake Borgne into the IHNC raised the water levels within the IHNC and then flowed north into Lake Pontchartrain. This precipitated the third phase of the disaster, as numerous failures and breaches occurred along the banks of the GIWW/MRGO and IHNC channels.

Fig. 2 shows a hydrograph of water elevations produced at five locations within the IHNC waterway as the storm surge was pushed westward from Lake Borgne through both the GIWW/MRGO and IHNC channels (IPET 2007). The storm surge rose at a moderate pace until it reached an elevation of approximately +5 ft (MSL) at approximately 10:00 p.m. on August 28, then it rose more rapidly over the next 11 h to a maximum elevation of approximately +14 to +14.5 ft (MSL) at approximately 8:45 to 9:00 a.m., after which it subsided relatively quickly. The dip in the rising hydrograph at one of the stations (where Highway I-10 Bridge crosses the IHNC) and the partial dip in a second gauge (also adjacent to the I-10 Bridge) were caused by a localized temporary drawdown due to the occurrence of a breach in that vicinity at approximately 5:00 a.m. The Highway I-10 Bridge is located immediately north of the two breaches labeled as Points *A* and *B* in Fig. 1. These two breaches are the most likely candidates for the source of this localized drawdown, and they are associated with penetrations of a rail line through the levee perimeter on both sides of the IHNC. The localized and temporary drawdown did not appear to extend far from the I-10 bridge, and it is the gauge levels without dips, representing conditions farther to the

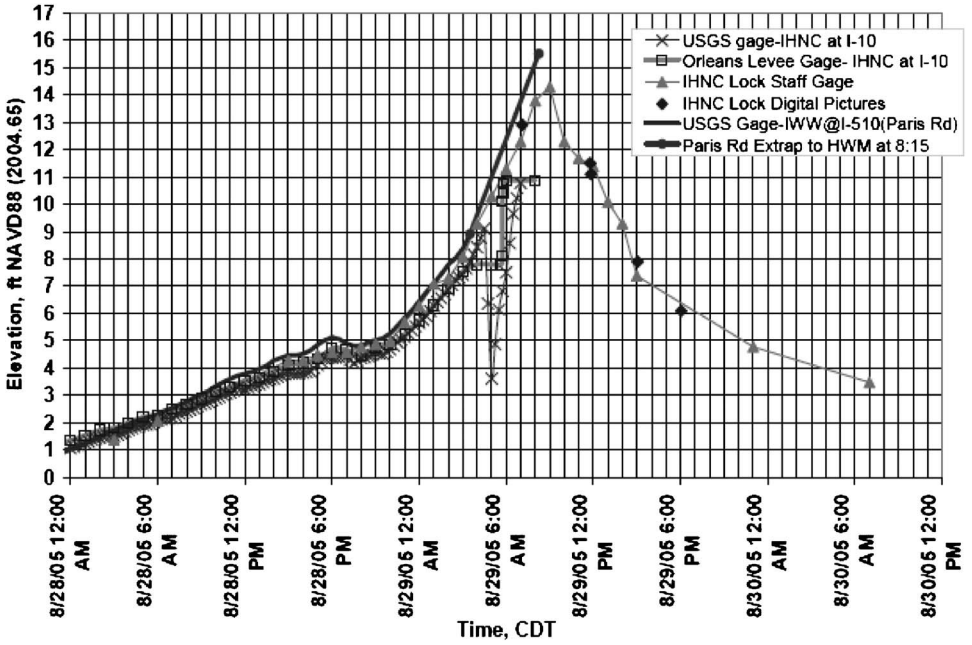


**Fig. 2.** Hydrographs showing measured (and photographed) water levels at gange stations along the IHNC (IPET 2007, Vol. V)

south within the IHNC, that will be the principal basis for discussions in the sections that follow.

## Failures along the GIWW/MRGO and IHNC Channels

The surge through the GIWW/MRGO and IHNC channels produced numerous breaches and partial breaches along both of these waterways. The following sections discuss key features common to some of the most important types of failures, and then present a more detailed examination of two catastrophic failures that occurred at the west end of the Lower Ninth Ward.

### *Failures at Transitions*

A majority of the failures along these two waterways occurred at transitions between two separate sections of the flood protection system, usually built at separate times as independent projects. At least 21 failures (breaches) and 10 additional partial failures occurred at such transitions (ILIT 2006; IPET 2006, Vol. V; ERP 2007; Van Heerden et al. 2006).

Fig. 3 shows a straightforward example of a transition between a full height earthen levee embankment section adjoining a half-height earthen embankment section topped by a sheetpile-supported concrete I-wall (floodwall). The elevation of the top of the I-wall shown on the left of Fig. 3 is approximately 1 ft higher than the top of the adjoining full-height earthen levee section. It was observed that the sections with significant "structural components" (e.g., concrete floodwalls, concrete gate structures with steel floodgates) consistently had slightly higher top elevations than adjoining earthen embankment sections (Baumy, private communication, 2005; ILIT 2006). The two adjoining and well-performing sections (levee reaches) in Fig. 3 are connected by a transition section that consists of a simple sheetpile wall section. The height of the top of this sheetpile wall is lower than either of the two adjoining levee or levee/floodwall sections, and overtopping thus occurred preferentially at this low spot. This overtopping flow eroded (scoured) a trench behind the back side of the sheetpile wall, and the lateral force of the floodwaters then pushed back against the now inadequately laterally supported sheetpile wall and produced the failure shown.

Failures at such transitions were common in this area and in other areas as well (e.g., Plaquemines Parish). Sixteen of the approximately nineteen full breaches and partially developed breaches along the GIWW/MRGO and IHNC waterways occurred at transitions between two flood defense sections; usually where structural sections joined with earthen embankments (ILIT 2006). There is clearly a need to recognize that these are flood protection systems, and that individual segments and components should combine seamlessly into an overall defense that does not have localized points of weakness (ILIT 2006; ERP 2007). Similarly, there is a need to place additional emphasis on the engineer-

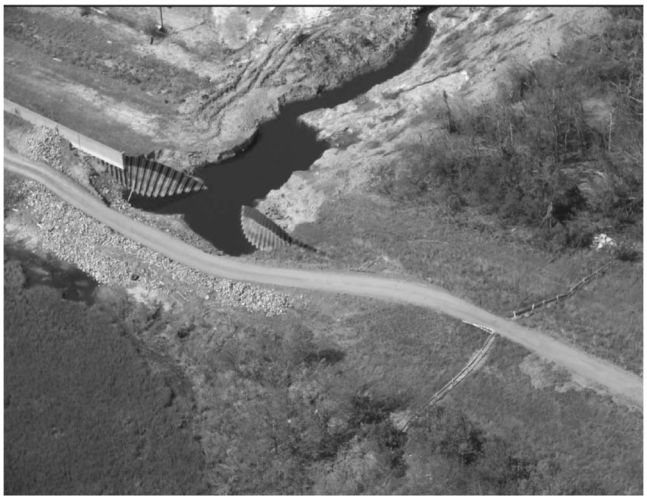

**Fig. 3.** An example of one of the numerous failures (breaches) that occurred at "transitions" between disparate, adjoining flood system elements. (From left to right: concrete floodwall, sheet pile wall, and earthen levee.)

ing design and construction of such transitions, as more than half of the approximately 53 breaches that occurred throughout the full region during this overall event occurred at transitions (ILIT 2006).

### *Failures at Penetrations*

One of the reasons for many of the transitions between differing types of adjoining flood protection system elements is penetrations, i.e., locations where a utility, pipe, roadway, rail line, or secondary navigable channel pass through the protective perimeter. This is often accomplished by means of gated concrete structures; or floodwalls with openings for rolling or hinged steel floodgates that can be closed during storm surges. These penetrations often pose an additional set of difficulties as they often represent locations where a collection of differing interests and differing authorities converge with overlapping responsibilities.

Seven of the failures and breaches, and six more of the partial failures, in this central region occurred at such penetrations/transitions, and there were at least nine additional failures at such penetrations/transitions at other locations throughout the overall region during this event (ILIT 2006; IPET 2007, Vol. V). Two of the most disappointing failures during Hurricane Katrina were the east bank and west bank crossings of the IHNC waterway by the CSX rail line (the two breaches indicated as Points *A* and *B* in Fig. 1). These same two sites had also failed previously during Hurricane Betsy in 1965, and so represented a failure to learn from that previous disaster.

The west bank crossing of the rail line (Point *A* in Fig. 1) represents an excellent example of the difficulties associated with complex penetrations. Fig. 4(a) shows the main breach at the site of the penetration of the rail line across the crest of the levee on the west bank of the IHNC, immediately to the south of the Highway I-10 Bridge. This photograph is taken looking east toward the IHNC, and the elevated Highway I-10 Bridge can be seen in the top left of the photograph. The rail line is adjacent to the highway bridge at ground level at the left of the photograph, and the steel drawbridge for the rails is in the raised position in the upper center of the photograph. At the time of this photograph, the breach had been partially repaired, and the newly compacted fill in the immediate foreground is infilling part of the original breach.

This is a complex multiple penetration, with the Highway I-10 Bridge crossing over the federal levee system immediately to the north of the rail crossing (at the left of the photograph), the rail line crossing over the top of the earthen levee and then crossing over a steel drawbridge (which is in a raised position at the center of the photo), and a road passing over the crest of the levee immediately adjacent to the rail line (the partially destroyed asphalt pavement at the right of the photograph) to provide access to Port of New Orleans facilities on the outboard (water) side of the federal levees. At least five agencies and bodies have mutually overlapping interests and jurisdictions at this site; the U.S. Army Corps of Engineers (USACE), the local levee board, the State Highway Department, the rail line, and the Port of New Orleans. In the course of our investigation, we were unable to determine who, if anyone, was in overall charge at this location prior to Hurricane Katrina's arrival.

The main failure and breach at this site occurred as a result of adverse interaction between the rail line and the adjacent port access roadway. The low spot at this site with regard to passage of water was the base of the pervious gravel ballast beneath the railroad tracks. Flow through this ballast appears to have eroded

(a)

(b)

**Fig. 4.** (a) Breach at a complex "penetration" through the federal levee system at the west bank crossing of the IHNC waterway by the CSX rail line; (b) concrete floodgate structure at the west bank IHNC crossing of the CSX Rail line

the soils beneath the adjacent port roadway. These soils consisted of poorly compacted, and highly erodeable, lightweight shell sands as evidenced by the eroded detritus strewn back behind the breach and by the material still in place beneath the partially destroyed asphalt cement pavement section shown in the photograph of Fig. 4(a) (ILIT 2006). As discussed in a companion paper (Seed et al. 2008a), these lightweight shell sand mixes, comprised of small mollusk shells and fine sands, are highly erodeable and represent an intrinsic hazard, especially when they are not provided with slope face protection to prevent risk of erosion due to frontal wave attack and overtopping and internal cut-offs to prevent through-flow. Conversely, the main (federal) levee embankment section was built with superior materials (compacted clay), but the USACE did not appear to have control of the selection of fill immediately beneath the roadway section.

A second problem occurred just to the left of the photograph of Fig. 4(a), immediately to the left of the person in Fig. 4(a), where the rail line passes through a concrete gatewall with a rolling steel floodgate. This location is shown in Fig. 4(b), this time looking west (away from the IHNC). The rail line passes through a concrete gatewall structure, and the people in this image are standing in the center of the gateway. A rolling steel floodgate is supposed to close this opening, but the steel floodgate had been damaged by a minor rail accident several months prior to Hurricane Katrina's arrival and had been taken away for repairs. An emergency levee

crest section was erected across the opening in the concrete gatewall using sandbags prior to Katrina's arrival, but it washed out during the storm, leaving another void in the perimeter defenses.

The lessons here are obvious, but they are also important. Penetrations are challenging both because they require transitions between different adjoining system elements and also because of overlapping interests and jurisdictions. If regional flood protection systems are to function safely and reliably, one organization should be in overall charge at such sites, and they must have sufficient authority to impose successful overall engineering solutions on behalf of public safety and the greater common good. Special attention should be paid to penetrations to ensure a reliable overall system of flood protection.

### *Partially Developed Breaches*

A large number of partially developed breaches occurred along the IHNC waterway, especially on the east bank of the IHNC at the west end of the New Orleans East protected basin. Most of these were erosional features where concrete floodwalls (often gatewalls for rolling steel floodgates) joined with earthen embankment sections. Erosion at the wall/embankment contacts, often at both ends of the gatewalls, was common. It should be noted that these partially developed breaches each began to erode and scour, but then the scouring stopped before a major breach could be fully eroded through the defenses. In our opinion, each of these partially developed breaches appeared to be capable of progressing to become a full breach, but they did not do so; in part because the New Orleans East protected basin was already infilling rapidly with floodwaters from numerous additional breaches at other locations, so that the inboard and outboard water levels had partially equilibrated before further scour occurred. Thus, most of these partially developed breaches were of little actual consequence in this disastrous event, but each might potentially have become features of greater significance if other, worse failures and breaches had not already occurred at other locations.

## Lower Ninth Ward

The two most significant breaches that occurred in the central region were located on the east bank of the IHNC, at the west end of the Lower Ninth Ward.

### *North Breach on the IHNC at the Lower Ninth Ward*

The first of these two breaches to occur was the north breach (at Location C in Fig. 1). Based on timing established by "stopped clocks" in the adjacent neighborhood and by an eyewitness, this breach occurred at approximately 5:30 a.m. (Van Heerden et al. 2006; IPET 2007, Vol. V; Consolidated Litigation 2008). The eyewitness saw the breach from a vantage point to the northwest and was looking across the waters of the IHNC, and hence he could not see what was occurring at the inboard (land) side of the levee and floodwall immediately prior to the breach.

Fig. 5 shows an aerial view of this feature. The levee runs from left to right across this photograph and the inboard side (landside) is at the bottom. This photograph was taken on October 5, 2006, and the interim outboard side repair embankment is nearing completion. The narrow, trench-like erosional channel through the breach has also been largely infilled at the time of this photograph. The toppled sheetpiles that had supported the concrete I-wall at this location can be seen just behind the nearly completed interim repair section. This was a relatively narrow feature, less than 90 ft in width, and unlike the more massive second failure that occurred approximately 3,000 ft to the south (as discussed in the section that follows) there was no evidence of sustained overtopping adjacent or near to this feature (ILIT 2006). The full depth of the breach feature was not determined prior to the commencement of emergency repairs.

Fig. 6(a) shows a cross section through this breach site, as modeled in the finite-element and limit equilibrium analyses. The cross section is based on two pre-Katrina borings located in close proximity to the breach performed for the original design studies, five borings and one CPTU probe performed by the IPET (2006) investigation, and two borings and one cone penetration test (CPTU) probe performed as part of our ILIT (2006) studies. Additional borings and CPT probes are available farther south along this frontage to further define stratigraphic units and their engineering properties.

As shown in this figure, the top of the concrete floodwall occurs at approximately Elev. +12.7 ft (MSL), and the steel sheetpile curtain supporting the concrete I-wall is tipped with its base extending to approximately Elev. −8 ft (MSL). The embankment crest occurs at an elevation of approximately +7.5 ft (MSL), and the levee embankment itself consists primarily of moderately compacted reddish brown clay fill. The embankment is underlain by marsh/swamp clays of relatively high plasticity (CH). These clayey swamp materials are underlain by a stratum of variable marsh deposits ranging from approximately 9 to 12 ft in thickness. These highly variable materials include peat deposits and variably interlayered clays and silts. The upper portion of these marsh deposits is more fibrous and peaty, and these are called out separately in Fig. 6(a) as the "upper marsh" stratum. The peats within the lower portion of the marsh stratum are generally more decomposed, but consist of similarly intermixed layers and lenses of peats, silts, and clays. The marsh stratum is, in turn, underlain by a relatively deep 30 ft thick layer of soft, light gray lacustrine or interdistributary clays of relatively high plasticity (CH). These are underlain by older beach sands and clays (Rogers et al. 2008), which represent stronger and more competent soils relative to the weaker overlying soil strata, and these older soil units were not involved in the failure (ILIT 2006). Figs. 6(a and b) also show the relatively extensive dredged hydraulic fill placed at the outboard side of the levee to create additional land for facilities on the outboard (water) side; these facilities had been abandoned and removed in the years prior to the hurricane.

#### Hypothesis No. 1: Underseepage-Induced Piping or Blowout

One of the potential types of failure modes examined at this site was underseepage-induced failure due to either (1) piping and erosion, or (2) hydraulic uplift/heaving (or "blowout") at the inboard toe. Transient flow analyses were performed using the finite-element program SEEP/W (Krahn 2004). Fig. 6(b) shows the finite-element mesh used for transient flow seepage analyses and Table 1 summarizes the parameters used to characterize the seepage characteristics of the critical strata. These parameters are based primarily on local experience and data from these soils, consideration of local practice, experience with similar soils in other regions, and engineering judgment. It was assumed in these analyses that the soils beneath the upper, compacted levee fill were saturated before the final relatively sharp rise in IHNC water levels began at about 10 p.m. on August 28, so that changes in pore pressure were essentially a pore pressure pulse, rather than requiring the passage of a large volume of water. The through-

**Fig. 5.** (Color) Aerial view of the north breach on the east bank of the IHNC, at the west end of the Lower Ninth Ward

passage of water pressures was further enhanced by the fact that the peaty marsh strata were partially capped by the less pervious overlying clayey swamp/marsh soils.

As shown in Fig. 6, the relatively short sheetpiles supporting the concrete floodwall along this frontage had been designed as cantilever support for the floodwall, and not as an underseepage cut-off, as it was assumed that the permeabilities of the foundation soils were sufficiently low that there would not be significant transmission of pore pressures beneath the floodwall during the relatively short duration of a hurricane-induced storm surge in the IHNC channel (USACE 1966). As a result, the sheetpiles did not extend deeply enough to cut off potential flow through the variably peaty upper marsh stratum.

The lateral (horizontal) hydraulic conductivity ($k_h$) of these peaty marsh deposits is thus a potentially critical issue here. The hydraulic conductivity of these layered marsh deposits is known to be highly anisotropic, and varies considerably as a function of composition, layering, and effective overburden stress. Unfortunately, it is the opinion of our investigation team that the "macro" scale seepage characteristics of these variably interbedded units cannot currently be satisfactorily characterized (at full field scale) with existing laboratory data. A parametric study was conducted, in which the $k_h$ values were varied from $10^{-3}$ to $10^{-6}$ cm/s (Table 1) to investigate: (1) the sensitivity of the calculated (time-dependent) propagation of underseepage-induced pore pressures to these variations; and (2) the ranges of $k_h$ that might prove critical for this site. Ranges of anisotropy of horizontal versus vertical hydraulic conductivities (i.e., $k_h/k_v$) of 10:1 to 50:1 were considered, but it was found that the horizontal conductivity was the dominant factor, and that variations in the anisotropy over this range had only a small effect on the results. The analyses reported in this paper use $k_h/k_v=10:1$ for these marsh units (ILIT 2006).

These transient flow analyses modeled the progressive rise in storm surge levels over the 24 h preceding the failure. Fig. 6(c) shows a close-up view of calculated seepage exit gradients as they would have existed at approximately 5:30 a.m. (with a canal water level of Elev. +10.5 ft, MSL) if the representative lateral hydraulic conductivity of the peaty marsh stratum had been $k_h=10^{-4}$ cm/s. This figure also shows the seepage gradient vectors; indicating that the principal passage of flow/pressure is through the marsh stratum, with high gradient vectors occurring around the base of the sheetpile curtain. For this particular scenario, exit gradients had become unsafe with regard to initiation of erosion and piping at an earlier stage of this analysis, with exiting gradients at and near to the inboard side levee toe reaching values greater than 0.6 (sufficient to begin piping for some of the lightweight soils in the toe region) as early as 4:30 to 5:00 a.m. In addition, the pore pressures beneath the thin surficial clay stratum

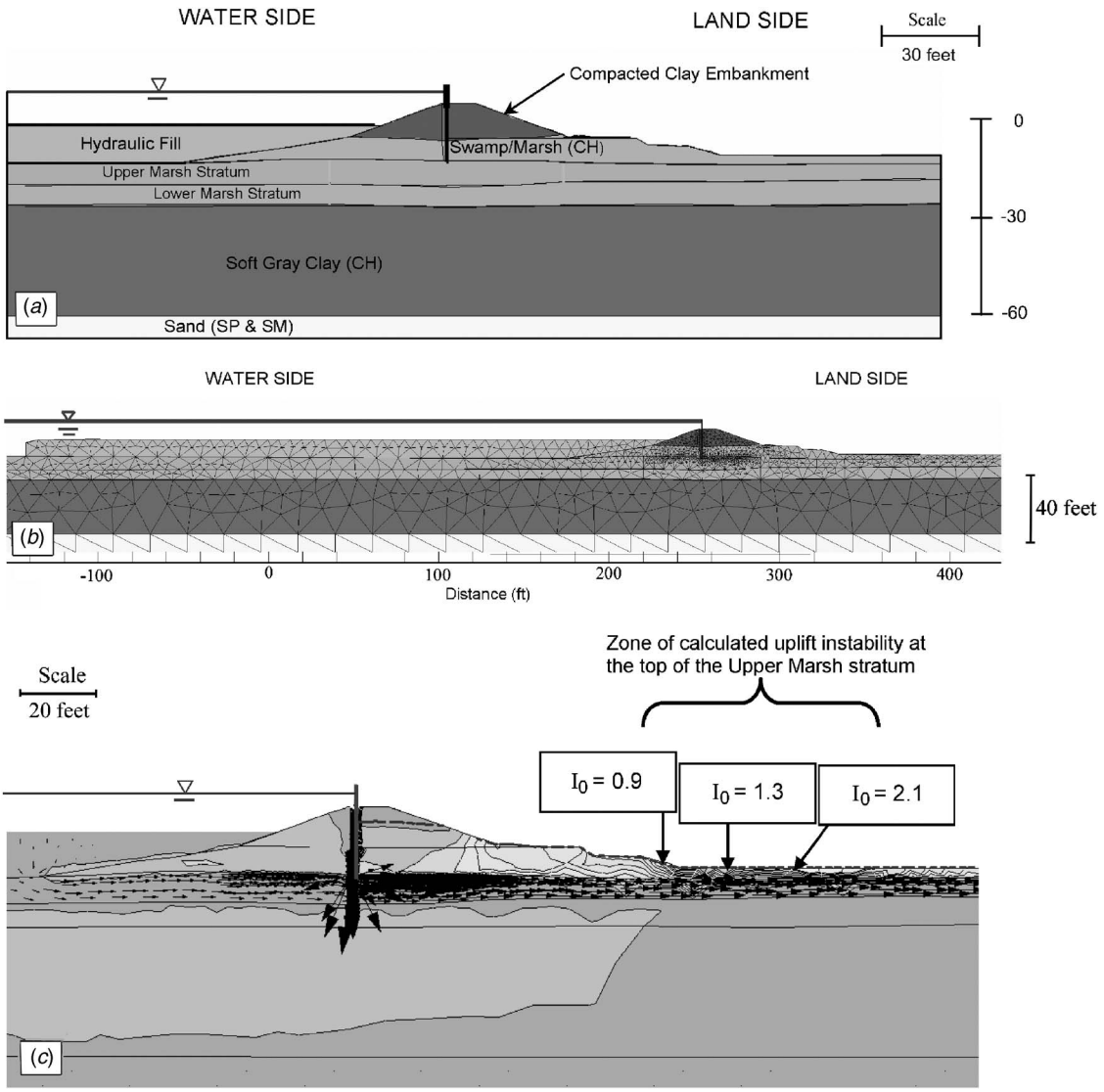


**Fig. 6.** (a) Cross section for analysis of the north breach, IHNC at the west end of the Lower Ninth Ward; (b) finite-element mesh for analysis of the north breach, IHNC at the west end of the Lower Ninth Ward; and (c) transient flow seepage analysis results showing equipotential lines (1 ft contours), seepage flow vectors, and exit gradients at 5:30 a.m., based on a lateral coefficient of permeability of the upper marsh strata of $k_h = 10^{-4}$ cm/s

**Table 1.** Principal Shear Strength and Permeability Parameters for the IHNC Breaches at the West End of the Lower Ninth Ward

| Stratum name | $\gamma_{unsat}$ (lb/ft$^3$) | $\gamma_{sat}$ (lb/ft$^3$) | $K_h$ (cm/s) | $K_v$ (cm/s) | Undrained shearing | | Drained shearing | | OCR[a] |
|---|---|---|---|---|---|---|---|---|---|
| Compacted fill (ML) | 115 | 115 | $10^{-6}$ | $10^{-7}$ | $c = 900$ lb/ft$^2$ | Ø = 0 | — | — | — |
| Swamp/marsh clay (CH) | N/A | 95 | $10^{-6}$ | $10^{-7}$ | | | — | — | Varies |
| Peaty Marsh | N/A | 80 | Varies[b] | Varies[b] | $(S_u/\sigma'_v)_{NC,DSS} \approx 0.24$, and $\lambda \approx 0.78$ | | $\mathbf{c' = 0}$ | Ø′ = 36° | Varies |
| Silt and mixed organics | N/A | 85 | $10^{-5}$ | $10^{-6}$ | $(S_u/\sigma'_v)_{NC,DSS} \approx 0.22$, and $\lambda \approx 0.8$ | | — | — | 2 |
| Soft gray clay (bay sound) | N/A | 105 | $10^{-6}$ | $10^{-7}$ | $(S_u/\sigma'_v)_{NC,DSS} \approx 0.24$, and $\lambda \approx 0.78$ | | — | — | Varies |

[a]OCR varies laterally across the domain as a function of overburden stress, and also varies over depth within these deposits.

[b]The horizontal permeabilities of the marsh deposits were varied over a range of $K_h = 10^{-3} - 10^{-6}$ cm/s in these studies, and vertical permeabilities were modeled as being between 10 and 20 times higher than horizontal permeabilities. For these finite-element analyses, the marsh permeabilities and canal water elevations were adjusted to provide pore pressures beneath the inboard levee toe approximately equal to those calculated in the transient seepage analyses performed separately by the finite-difference method.

immediately to the inboard (landside) of the levee toe also became potentially unsafe with regard to hydrostatic uplift (heave) of the less pervious soils overlying the marsh stratum at approximately that same point in time, so that hydraulic uplift (or "blowout") at the toe was likely to have been the first manifestation of this progressively evolving uplift/piping erosional failure mode.

The expected timing of the resultant failure is difficult to ascertain based on analyses of this type, as the rate at which piping erosion would then progress to full failure is difficult to predict. However, it is expected that the erosional piping would progress very rapidly back through the lightweight and highly erodeable marsh deposits, undermining the overlying strata and eventually the levee embankment. At some point, lateral stability failures of the retreating toe section would have occurred and further exacerbated this process. Although precise timing for this progression to failure cannot be established from these types of analyses, it is clear that they indicate the potential for underseepage-induced erosional (and/or uplift) failure as early as about 5:00 a.m. By varying $k_h$ of the marsh strata, we found that values greater than $10^{-5}$ cm/s are sufficient to produce unsafe exit gradients and also potential uplift pressures at the inboard toe at times between 4:30 and 5:30 a.m., corresponding well with the observed approximate time of failure. For values of $k_h \leqslant 5 \times 10^{-6}$ cm/s, unsafe exit gradients and unsafe uplift pressures do not develop at the inboard toe region until later points in time.

These analyses thus strongly suggest the possibility that the mechanism of failure at this site may have been underseepage-induced erosion and piping, possibly exacerbated by hydraulic uplift at the inboard levee toe, but only if the lateral hydraulic conductivity ($k_h$) of the variable marsh stratum was greater than $10^{-5}$ cm/s.

**Hydraulic Conductivity of the Marsh Strata.** The hydraulic conductivities of these marsh strata decrease with effective overburden stress, and locally available data for samples of similar marsh deposits in the region obtained from borings and tested in the laboratory show hydraulic conductivity ranges on the order of $k_v \approx 10^{-6}$ to $10^{-7}$ cm/s for marsh deposits in this region under significant overburden pressures (i.e., beneath the centerline of the levee embankment) (Boutwell, private communication, 2006). The few laboratory test data available show (1) similar tends with effective overburden stress; and (2) higher $k_h$ values at the same overburden stresses (i.e., $k_h/k_v \gg 1$). This finding is supported by data regarding $k_v$ and $k_h$ values for similar, peaty marsh deposits from other regions (e.g., Bear 1972; Shepard 1989; Bell 2000; Bechwith et al. 2002, 2003; Hogan et al. 2006; Mesri and Ajlouni 2007; URS Corp. 2007). These studies indicate that the lateral hydraulic conductivity of peaty soils generally varies over a range of $10^{-2}$ to $10^{-7}$ cm/s, with the higher values corresponding to peats at lower effective overburden stresses. Anisotropy is very pronounced, with $k_h$ values generally significantly higher than $k_v$ values.

It is our view that individual (small scale) samples obtained from borings and then tested would serve poorly to characterize the overall lateral permeabilities of the variably interlayered deposits at this site. Support for this included two historic, field-scale observations: (1) There is a well-established history of seepage problems along this frontage prior to Katrina (Consolidated Litigation 2008) involving accumulation of water during episodic (lesser) high water events, and (2) records indicate that an experienced contractor attempted but was unable to successfully dewater an excavation for construction of new pumping facilities immediately north of the north breach; this was attributed to unexpectedly high conductivity through the peaty marsh strata (Consolidated Litigation 2008). Moreover, Team Louisiana, the first investigation team to reach this site after the hurricane reported observing several apparent boils inboard of the levee toe, just to the south of the north breach. Finally, as discussed later in this paper, an underseepage-induced crevasse splay (erosional feature) occurred at the location of the massive south breach, and under very low reverse flow gradients as the last of the floodwaters drained back into the IHNC beneath the interim repair section at that site.

Overall, it was the judgment of our investigation team that $k_h$ values of the peaty marsh stratum may well have been as high as $10^{-4}$–$10^{-5}$ cm/s, at least at localized sections along this frontage.

**Hydraulic Conductivity of the Outboard Side Hydraulic Fill.** An additional question relating to the feasibility of underseepage as a potential failure mechanism at this breach site is the question of the hydraulic conductivity of the hydraulic fill that had been placed at the outboard side of the levee section to create land for outboard side facilities, as shown in Fig. 6(b). If these fill soils were consistently of low permeability, then they would have acted as an outboard side impervious blanket and would have largely eliminated any possibility of significant underpassage of pore pressures and flow beneath the levee during the storm surge.

These outboard side fill materials are poorly characterized, and we were unable to obtain citable data regarding these as they are currently an issue of contention in the ongoing civil litigation regarding this site (Consolidated Litigation 2008). This fill was dredged from the base of the IHNC and then placed hydraulically, but we have been unable to obtain documentation suggestive of good control of materials during this process. Both clays and sands would have been available, depending on the depths from which these soils were dredged. IPET performed several borings in this outboard side hydraulic fill, and reported that it was primarily clayey material at those locations. Visual observations and manual classification of portions of this material accessible after the hurricane by our own investigation team showed the material to contain significant sandy zones at those points that we could access (near to the outboard side levee toes along this frontage).

Evidence and documentation now coming to light as part of the ongoing litigation show that a number of holes were excavated in this hydraulic fill during removal (and environmental cleanup) of the outboard side structures and facilities several years before Hurricane Katrina's arrival. One of the most noteworthy examples is a large hole where a railroad tanker car had been buried within the original hydraulic fill to serve as a fuel tank for the outboard side facilities. This tanker had been located closely outside of the large breach that occurred approximately 3,000 ft further to the south that is the focus of the latter portion of this paper (near to the north end of that breach, within the breach frontage). The hole formed by excavation to remove that tanker appears to have been infilled with pervious gravelly and sandy soils. In addition, the adverse history of seepage problems along this frontage would also suggest that the outboard side hydraulic fill does not appear likely to function consistently as an impervious blanket. Accordingly, relatively unimpeded flow through this fill (at least local to the two breaches) was modeled in our analyses.

### Hypothesis No. 2: Deep, Semirotational Stability Failure through the Soft Foundation Clays

The second potential failure mechanism investigated at this site was a semirotational lateral stability failure, with a basal shear

surface passing primarily through the soft gray clays underlying the upper marsh deposits. This failure mechanism was also investigated by the IPET investigation; however, the approaches taken to characterize the shear strength characteristics of the deep layer of soft gray clays by the investigation teams differed in several ways including: (1) weighting of available laboratory (UU-TX) versus field test (CPTU) data; (2) procedures for addressing the effects of variations in effective overburden stresses at various locations at and near to the inboard side levee toe; and (3) our investigation found the clay stratum to be significantly overconsolidated at its top (apparently due to desiccation) and moderately overconsolidated near its base, while the IPET interpretation considered the unit to be normally consolidated throughout.

Seed et al. (2008c) presents a detailed explanation of the processes used for derivation of shear strengths for these types of clay and marsh strata at a site with very similar stratigraphy. In summary, our approach recognized the problems and uncertainties associated with use of UU-TX data for these types of soils, and so concentrated initially on the use primarily of CPTU data. Site-specific and material-specific CPT tip factors ($N_{kt}$) were developed for evaluation of undrained shear strengths for this clay unit, and the available CPT data (from the four profiles within closest proximity to the failure location) were then used to perform an inverse (SHANSEP-type) regression as suggested by Pestana to simultaneously develop estimates of the vertical profiles of overconsolidation ratio (OCR) and undrained shear strength ($s_u$) versus depth at various locations (ILIT 2006). Good agreement was found between these and apparent profiles of $s_u$ versus depth at various locations based on the conjugate UU-TX data available from both the pre-Katrina investigations and the various post-Katrina investigations as well as with data from other sites with similar materials (ILIT 2006).

Beneath the levee crest, where the effective overburden stresses were greatest due to the thick levee fill, the clay stratum was found by our approach to be nearly normally consolidated over most of its depth. However, the soil shear strengths beneath the inboard side levee toe, and further inboard (beneath the free-field), are most critical for this potential failure mode. In this critical region we found the clay stratum to have a significant overconsolidation profile near the top (representative of a desiccation profile due to periodic exposure during the progressive geologic accretion of sediments at this site), and the clay stratum was also found to be moderately overconsolidated near its base; probably due to aging and secondary compression of the older soils near the bottom of the relatively thick stratum (ILIT 2006). This profile was similar to the profile of the similar soft gray clay deposit at the 17th Street Canal breach site (Seed et al. 2008c).

Our modeled ratio of $s_u/\sigma'_v$ reflects the application of a number of empirical adjustments to account for anisotropy and the direct simple shear (DSS) conditions that would dominate this mode, and also for the sensitivity of these clays (ILIT 2006). Specifically, we derived a ratio of $(s_u/\sigma'_v)_{NC,TX} \approx 0.31$ for normally consolidated material under triaxial conditions, after which we applied a set of empirical modifications for (1) stress path and anisotropy; and (2) sensitivity to develop an estimated ratio of $(s_u/\sigma'_v)_{NC,DSS} \approx 0.24$ for the direct simple shear conditions dominant for this potential failure mode at this site. These empirical adjustments were similar to those applied by the IPET investigation. A SHANSEP coefficient of $m \approx 0.78$ was used to define the variation of $(s_u/\sigma'_v)_{DSS}$ as a function of overconsolidation ratio (OCR). These values of $(s_u/\sigma'_v)_{NC,DSS}$ and $m$ were found to be in excellent agreement with data for similar materials compiled by

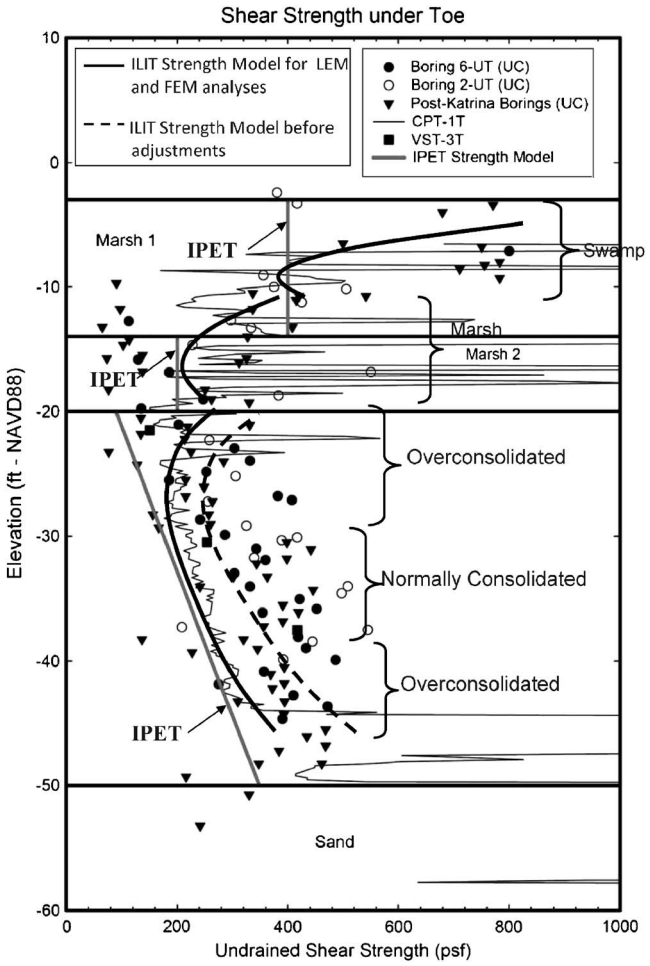


**Fig. 7.** ILIT model for shear strengths beneath the inboard side levee toe; north breach, IHNC at the west end of the Lower Ninth Ward (adapted from IPET 2007, Vol. V)

Ladd and DeGroot (2003), and also with the results from similar deposits at other key sites in the New Orleans region.

The heavy black line in Fig. 7 shows a profile of $(s_u/\sigma'_v)_{DSS}$ used at a lateral location directly beneath the contact of the inboard side levee toe and the nearly horizontal adjacent ground surface within this critical clay stratum in our own studies [these profiles continued to vary somewhat further beneath the levee, and further toward the inboard (free field) side, as a function of varying overburden stresses]. The heavy dashed line in Fig. 7 shows the profile of $s_u$ versus depth determined by our studies (prior to adjustments for DSS shear conditions); this increases linearly versus depth in the middepth region where the clays are normally consolidated, but this profile shows higher strengths at the top and bottom of this clay stratum representing the variable OCR profiles in these zones. This strength profile is in good agreement with the available UU-TX data. The heavy solid line then shows the final profile of $s_u$ versus depth, after empirical adjustments (reductions), that was actually used for the limit equilibrium stability analyses performed (and also for finite-element analyses as well). The adjacent linear trend, showing strength increasing linearly versus depth, was the alternate interpreted strength profile used in the corresponding IPET (2006) analyses.

Our characterizations of shear strengths in the marsh strata and in the overlying marsh/swamp strata also depended heavily on the use of CPTU data, and cross correlations with available empirical

**Table 2.** Summary of Soil Model Parameters Used in PLAXIS Analyses for the IHNC South Breach (East Bank)

| Stratum name | PLAXIS soil model | Shearing type[a] | $\gamma_{unsat}$ (pcf) | $\gamma_{sat}$ (pcf) | $k_h$ (ft/day) | $k_y$ (ft/day) | $\nu$ | $E_{ref}$ (psf) | $c_{ref}$ (psf) | $\varphi'$ (deg) | | | | |
|---|---|---|---|---|---|---|---|---|---|---|---|---|---|---|
| Compacted fill (ML) | Mohr Coulomb | Undrained | N/A | 115 | 0.0028 | 0.00028 | 0.35 | 234,000 | 900 | 0.001 | | | | |
| Stratum name | PLAXIS soil model | Shearing type | $\gamma_{unsat}$ (pcf) | $\gamma_{sat}$ (pcf) | $k_h$ (ft/day) | $k_y$ (ft/day) | $\lambda^*$ | $\kappa^*$ | $\nu_{ur}$ | $Ko_{nc}$ | $M$ | $c_{ref}$ (psf) | $\varphi'$ (deg) at $p_{ref}$[d] | OCR[b] |
| Fat clay (CH) | Soft soil | Undrained | N/A | 95 | 0.0028 | 0.00028 | 0.17 | 0.03 | 0.15 | 0.63 | 1.24 | 0.001 | 22 | varies |
| Marsh | Soft soil | Undrained | N/A | 80 | Varies[c] | Varies[c] | 0.21 | 0.033 | 0.15 | 0.6 | 1.9 | 0.001 | 36 | varies |
| Silt | Soft soil | Undrained | N/A | 85 | 0.03 | 0.003 | 0.1 | 0.02 | 0.15 | 0.61 | 1.27 | 0.001 | 23 | 2 |
| Stratum name | PLAXIS soil model | Shearing type | $\gamma_{unsat}$ (pcf) | $\gamma_{sat}$ (pcf) | $k_x$ (ft/day) | $k_y$ (ft/day) | $\nu$ | $E_{ref}$ (psf) | $c_{ref}$ (psf) | $\varphi'$ (deg) | | | | |
| Soft gray clay (bay sound) | Mohr Coulomb | Undrained | N/A | 105 | 0.0028 | 0.00028 | 0.3 | 1,000,000 | 800 | 0.001 | | | | |

[a]These soils were modeled as "drained" during consolidation under the embankment fill loads, but were then modeled as "undrained" during the short-duration loading represented by the rapid storm surge rise within the canal.

[b]OCR varies laterally across the domain as a function of overburden stress, and also varies over depth within these deposits.

[c]The horizontal permeabilities of the marsh deposits were varied over a range of $K_h = 10^{-3} - 10^{-6}$ cm/s in these studies, and vertical permeabilities were modeled as being between 10 and 20 times higher than horizontal permeabilities. For these finite-element analyses, the marsh permeabilities and canal water elevations were adjusted to provide pore pressures beneath the inboard levee toe approximately equal to those calculated in the transient seepage analyses performed separately by the finite difference method.

[d]Friction angle for soft soil model defined at $p_{ref} = 1$ atm.

relationships for similar soils at other locations. Once again, we performed an inverse SHANSEP-based regression of the available data, and concluded that these two upper units (the marsh and the overlying marsh/swamp clays) both exhibited classic overconsolidation profiles typical of "stands" during the progressive accretion of these deposits. Fig. 7 shows our strength model (at a location directly below the termination of the inboard side levee toe) for these units. These clearly show our interpretation regarding a classic pair of desiccation profiles in both units, and also the somewhat lower strengths (the vertical lines in these two strata in Fig. 7) used in the IPET analyses.

Table 2 summarizes the shear strength parameters used in limit equilibrium analyses of this potential semirotational failure mode by our studies. It is noted that both the IPET and ILIT used similar properties to characterize the strengths of the engineered levee embankment fill, based on the limited UU-TX data available, and that these do not significantly affect the results of the stability analyses as the embankment would have largely displaced monolithically atop a shear failure surface dominated by the underlying soft clays in this hypothetical potential failure mode.

Both investigation teams performed limit equilibrium analyses to assess the factor of safety (FS) for a potential semirotational failure through these soft gray clays, and both assumed the formation of a water-filled gap on the outboard side of the sheetpiles/I-wall, between the sheetpiles and the soils, and applied full pore pressures laterally against the sheetpiles/I-wall to push the inboard side of the levee embankment section toward the inboard (land) side. Our analyses were performed using Spencer's method (1967), with the computer program SLOPE/W (Krahn 2004), and the results for the critical surface were cross-checked both by hand and using the program UTEXAS4 (Wright 1999).

Fig. 8 shows the most critical potential failure surface found by our analyses for this potential deep, semirotational failure mode, and for an IHNC water level of Elev. +10.5 ft (MSL); the conditions present at approximately 5:30 a.m. when the actual failure occurred. The critical failure surface shown in Fig. 8 is similar to the most critical failure surface found by the IPET studies (IPET 2007). Although both studies found similar geometries for the most critical potential failure surface, the calculated levels of stability differed somewhat between the two investigations. Our characterization of strengths within the soft gray clays and overlying marsh and swamp strata, including the additional strength due to the overconsolidation profiles found within these strata, resulted in a somewhat higher calculated FS values when compared to the IPET findings. We computed the factor of safety for the most critical failure surface of Fig. 8 to be approximately FS = 1.18, for a canal water level of +10.5 ft, whereas IPET found the FS to be 1.03 for that same canal water level.

In addition, we note that these are two-dimensional plane strain analyses, and that they likely significantly underestimate the actual three-dimensional (3D) factor of safety due to the unusually narrow and deep shape of the actual field failure (low aspect ratio) and the cohesive strength that would have been mobilized along the sides of this narrow feature. Our best estimate of the actual factor of safety is therefore approximately 5–10% higher, in order to account for these 3D effects, resulting in a best-estimated overall FS $\approx$ 1.24–1.30. This represents an apparently stable condition, but we acknowledge that uncertainties might still have permitted the occurrence of such a deep rotational failure at this IHNC water level. Nevertheless, even if we consider only the two-dimensional FS of 1.18 for the critical failure

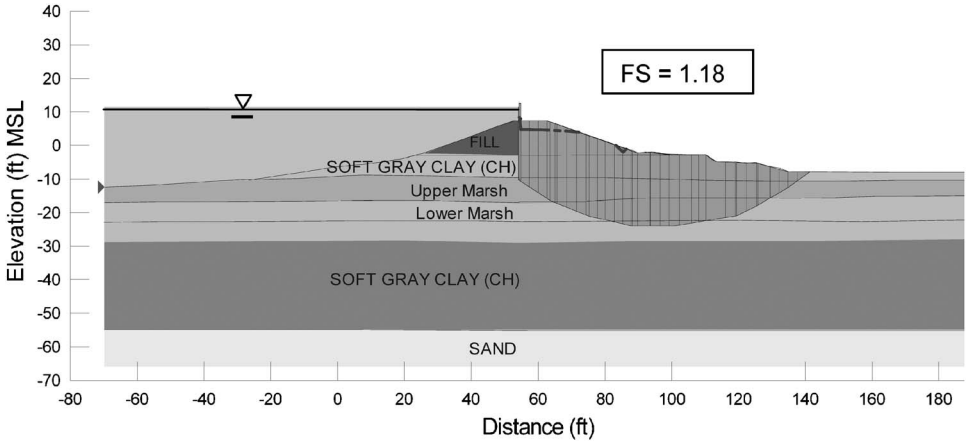


**Fig. 8.** Calculated minimum factor of safety for deep, semirotational failure at the north breach, IHNC at the west end of the Lower Ninth Ward with surge height at Elev. +10.5 ft (MSL)

surface for this mechanism, we judge this to be less likely than the underseepage and piping mode of Hypothesis No. 1.

More important, it should be noted that the deep rotational mode of failure *would* have become more critical if the levee and I-wall section had remained in place until the IHNC water level reached its eventual peak within the IHNC at an elevation of approximately +14 ft, MSL. Our analyses indicate marginal stability (FS ~ 1) for this failure mode at that higher water stage.

### Hypothesis No. 3: Translational Stability Failure due to Underseepage-Induced Strength Reductions

The third potential failure mechanism studied was a potential lateral translational instability, with shearing largely within the "marsh" due to the combined effects of: (1) lateral water pressures acting against the face of the sheetpiles/I-wall; and (2) reduction in shear strengths at the top of the marsh stratum due to underseepage-induced increases in pore pressures (and resulting decreases in effective stress) at this location.

A detailed study and analysis of exactly this mode of potential failure is presented in the next section of this paper for the massive second breach that occurred approximately 3,000 ft to the south (the South Breach), and to save space readers are referred to that section (which had very similar soils and stratigraphy) for details of this type of analysis. The important findings here were: (1) At each IHNC water level, and for each assumed value of $k_h$, the potential failure mode of Hypothesis No. 1 (underseepage-induced piping and/or uplift and blowout) as discussed previously provided a more critical situation (lower FS), and (2) the analyses of this mode (underseepage-induced lateral translational instability) produced FS = 1.11, 1.20, and 1.34 for canal water elevations of +10.5 ft, MSL (the conditions at 5:30 a.m. when the breach occurred) when coupled with values of $k_h = 10^{-3}$, $10^{-4}$, and $10^{-5}$ cm/s, respectively.

Based on these analyses, it was concluded that this potential failure mode could not be fully excluded, but that (like the mode of Hypothesis No. 2) it was a less likely mode than the underseepage-induced erosional failure of Hypothesis No. 1. Similarly, once again this potential failure mode would have represented a more critical condition if the section had remained in place for another 3 h (until the peak rise in the IHNC to Elev. +14 ft, MSL at approximately 8:45 a.m.), by which time factors of safety of less than 1.0 would have occurred for this mode for all values of $k_h \geq 10^{-5}$ cm/s.

**Summary of the Prevailing Failure Mechanism.** As described in the preceding sections, it was our investigation's conclusion that three potentially feasible failure mechanisms were present and operating at this site, rendering the determination as to which mechanism occurred first and actually caused the failure to be somewhat challenging. The analyses presented would slightly favor the mechanism of Hypothesis No. 1 (underseepage-induced failure due to piping, likely exacerbated by initial uplift and blowout at the toe), but these are not fully conclusive, due in large part to uncertainties associated with $k_h$ of the variable marsh strata. In the end, it is the confluence of these analyses, and the actual field observations, that should jointly form the basis for assessment of the most likely failure mechanism.

The mechanism of underseepage-induced uplift and erosional piping failure best fits the narrow geometry of the observed failure (and closely matches the similarly narrow geometry of the failure near the south end of the London Avenue Drainage Canal, which was also judged most likely to be an underseepage-induced piping failure; Seed et al. 2008b; IPET 2007). The available field information and local observations regarding apparent permeability characteristics and the local history of underseepage problems prior to Katrina also lend support for this mechanism. In addition, the other two potential mechanisms considered show higher (and apparently stable) FS values at the time (and water elevation) at which this failure occurred.

An underseepage-induced failure would require the flow (or at least the pore water pressure) to defeat the apparent waterside blanket represented by the hydraulically placed fill at that location. Given the variable apparent nature of that fill, its relatively poor documentation, voids apparently introduced during removal of structures and facilities prior to Katrina, and the history of seepage problems along this frontage, it appears likely that the outboard side hydraulic fill was not fully effective in preventing underseepage along this full frontage.

Some debate and differences of opinion continue to persist within our investigation team, but the majority consensus is that underseepage-induced failure and piping (likely exacerbated by hydraulic uplift), likely also exacerbated by localized evolution of lateral instability as the toe geometry progressively degraded, represents the most promising overall candidate mode, and that the other two modes (lateral semirotational instability failure through

**Fig. 9.** (Color) Oblique view of the (south) levee breach at the Inner Harbor Navigation Canal into the lower Ninth Ward

the top of the soft gray clays, and lateral translational/semirotational instability due to underseepage-induced strength loss) cannot be fully discounted.

### *South Breach on the IHNC at the Lower Ninth Ward*

As shown in Fig. 1 (Location D), a second massive failure and breach occurred approximately 3,000 ft to the south of the breach discussed in the previous section. This was one of the largest and best-known failures to occur during Hurricane Katrina. This breach occurred at approximately 8:30 a.m., with the water level in the adjacent IHNC at approximately +14 to +14.5 ft (MSL).

Fig. 9 shows an oblique aerial view of this south breach, which was approximately 950 ft in length. A large barge was washed in through this very long feature, and is visible in this photograph near to the top of the image (just inboard of the south end of the breach). The toppled and displaced sheetpile wall is also clearly visible; the sheetpiles remained interlocked throughout the severe inflow and scour caused by the breach, and the sheetpile curtain (although stretched and extended to a length of approximately 1,300 ft as the flanges were stretched and straightened out) is still contiguous over its full length. The concrete floodwall atop the sheetpiles could not match this level of extensile ductility so most of the concrete I-wall panels spalled off of the top of the sheetpile curtain during this failure.

As shown in the left half of the photograph of Fig. 9, the inboard side community was devastated by the heavy rush of water through this breach; the homes of the first several blocks have been stripped from their foundations and scattered across the community. At the time of this photograph (September 30, 2006), the initial interim closure embankment on the outboard side of the large breach had been largely completed (the lighter colored new embankment section in the right-center of the photograph).

The first question to answer was whether the barge caused the breach or was it drawn in through a breach that was already open. Fig. 10 shows a close-up view of the top of the concrete floodwall at the south end of the breach. The concrete floodwall along the top of the sheetpile curtain across the full rest of the width of this large breach was largely spalled off of the tops of the sheetpiles in extension as the sheetpiles were pulled by extensile/tensile forces. The south end of the breach (Fig. 10) was the only location where the concrete floodwall was crushed by compressive impact. In addition, a large dent on the left side of the barge, near the bow, and a scrape on its base at that location, appeared to correlate well

**Fig. 10.** Close-up view of crushed (impacted) concrete floodwall at the south end of the south breach at the east bank of the IHNC at the west end of the Lower Ninth Ward

with the south end impact site shown in Fig. 10. Finally, as described later, geo-forensic studies performed as part of our investigation show that this section would have been expected to fail without barge impact. It was concluded by this investigation that the barge was most likely drawn in through a breach that was already open, and that it impacted at the extreme south end of the breach as it passed inland through the (already open) breach.

Fig. 11 shows a trench behind the concrete floodwall at the south end of the breach. This photograph is taken looking north, and the large barge can be seen in the background of this image. As canal waters overtopped and passed over the top of the floodwall, they eroded this trench, reducing the lateral support for the floodwall and its supporting piles. The IPET investigation (IPET 2007, Vol. V) concluded that this directly caused the failure, as the raised waters in the canal pushed the then insufficiently laterally braced wall sideways toward the inboard (protected) side.

Fig. 12 shows a cross section through the breach section. The top of the concrete floodwall at this location is at approximately Elev. +12.7 ft (MSL). The foundation stratigraphy at this section

**Fig. 11.** Eroded trench at the rear (inboard) side of the floodwall at the south end of the south breach at the east bank of the IHNC at the west end of the Lower Ninth Ward

is similar to that of the north breach discussed previously in this paper. The clayey levee embankment sits atop primarily gray swamp/marsh clays (CH) with occasional plastic silt strata, but there are two significant marsh deposits in the upper foundation as well. As shown in Fig. 12, the sheetpile curtain supporting the concrete floodwall is again very short, with its base at Elev. −8 ft (MSL), and fails to cut off flow through the second (main) marsh layer. As with the nearly adjacent north breach, the marsh layer is a variably interbedded layer of organic silts, clays, and peats. The $k_h$ of this ensemble is variable, and there is a well-established history of underseepage problems along this overall levee frontage (ILIT 2006; Van Heerden et al. 2006; Consolidated Litigation 2008).

Transient flow analyses showed that the rising storm surge in the canal was likely able to be at least partially transmitted to foundation soils beneath the inboard side levee toe. The storm surge rose slowly at first, cycling with tides over the several days preceding the storm's arrival, and then the rate of water level rise increased as the eye of the storm approached more closely, raising water levels from Elev. +4.5 ft to their full peak at approximately Elev. +14 to +14.5 ft (MSL) over a 15 h period, and overtopping the concrete floodwall by a bit more than a foot. Finite-element analyses were performed, again using the program SEEP-W, to model the progressive rise in IHNC water levels shown in Fig. 2. Properties for the key strata were modeled in the same manner as was discussed previously for the nearby north breach and are summarized in Table 1.

Fig. 13(a) shows equipotential contours (contoured in 1 ft increments of head) and seepage vectors for transient flow analyses of conditions just as the canal water levels reached Elev. +14 ft (MSL) at approximately 8:30 a.m. Once again the marsh stratum was assumed to be initially saturated prior to the final rise in storm surge level. The equipotential contours shown in Fig. 13(a) are those calculated based on an assumed value of $k_h = 10^{-4}$ cm/s for the marsh stratum. Fig. 13(b) shows pore pressures calculated at the top of the marsh stratum, directly beneath the inboard side levee toe [directly beneath Point *D* in Fig. 13(a)] based on transient flow analyses modeling the time series of storm surge rise (see Fig. 2), and using a range for the marsh stratum of $k_h = 10^{-3} - 10^{-6}$ cm/s. The fully developed steady state seepage pore pressure at this location (at the top of the marsh stratum, directly beneath Location D) would have been 1,080 lb/ft$^2$ if the maximum canal water level of Elev. +14 ft (MSL) had remained in place long enough as to permit the establishment of steady state flow conditions.

Fig. 13(b) shows porewater pressures calculated over the last 4 h before the surge peaked at about 8:45 a.m. As shown in this figure, the fraction of the steady state pore pressure that actually accrues at this location is affected by the $k_h$ of the marsh stratum. For values of $k_h = 10^{-3}$, $10^{-4}$, $10^{-5}$, and $10^{-6}$ cm/s, the fraction of the full steady state pore pressure achieved by transient flow at this location would have been on the order of 92, 84, 78, and 73% of the steady state pore pressures, respectively. This overstates the degree of pore pressure transmission due to the transient rise in canal water level, however, as the pore pressures shown in Fig. 13(b) also include the initial pore pressure present at this location prior to the final storm surge rise. Subtracting out the initial pore pressure as it existed approximately 24 h before the final storm surge rise, the fraction of the steady state pore pressure change (due to storm surge rise) transferred to the top of the marsh beneath Point *D* was calculated to be on the order of 83, 61, 49, and 38% for values of $k_h = 10^{-3}$, $10^{-4}$, $10^{-5}$, and $10^{-6}$ cm/s, respectively.

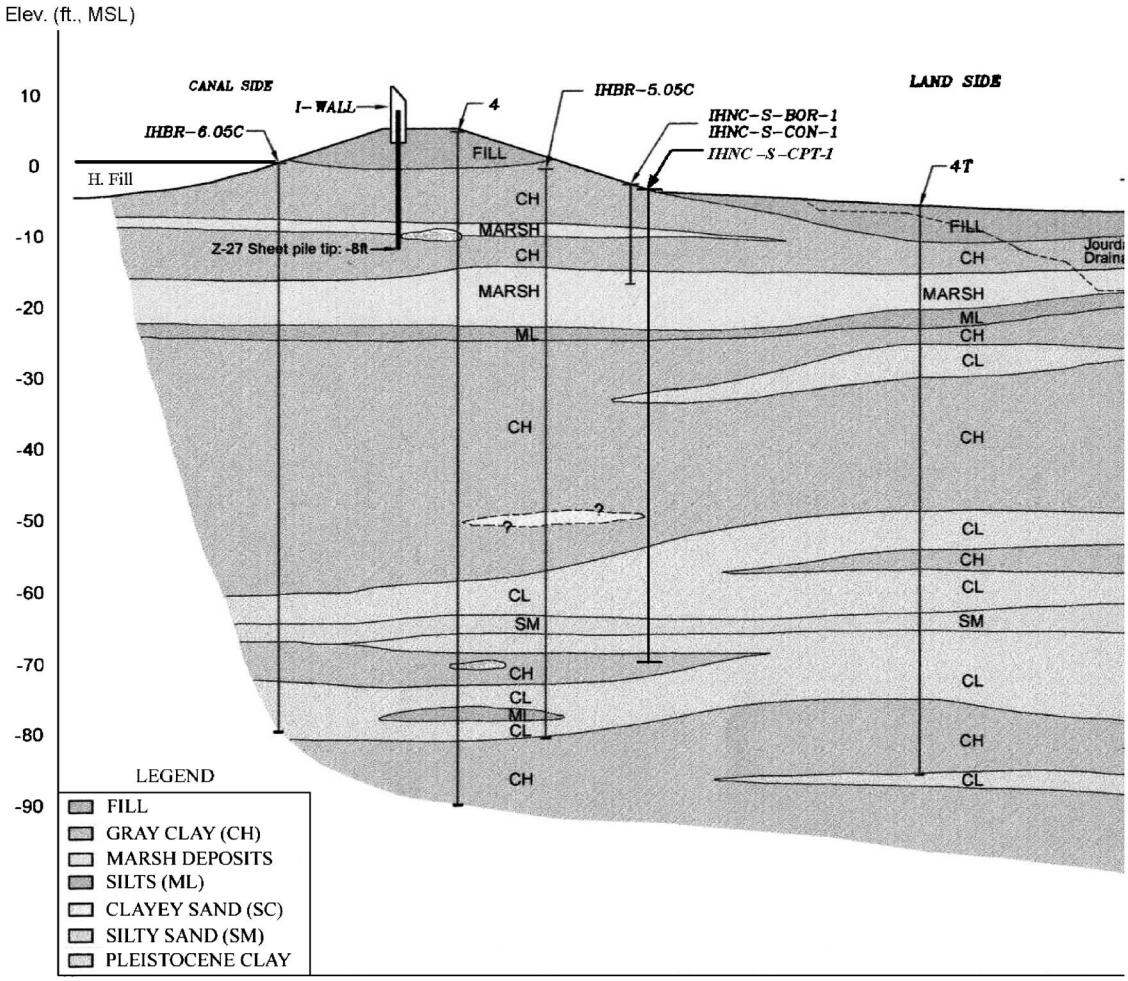


**Fig. 12.** Cross section through the large south breach on the east bank of the IHNC, at the west end of the Lower Ninth Ward

It should also be noted that the pore pressures shown in Fig. 13(b) correspond to the gapped case, wherein it is assumed that a gap opens between the sheetpiles and the levee embankment soils on the waterside as the canal water reaches an elevation of approximately +10 to +11 ft (MSL), as such gapping was suggested by finite-element analyses performed to model the behavior of this section (ILIT 2006). The effect of this opening of a gap, in part, was to permit direct entry of high water pressures at the base of the sheetpile curtain during the later stages of the storm surge rise, and this also adds a bit to the calculated overall pore pressure rise beneath the inboard side of the levee embankment.

Exit gradients at the toe were calculated to be marginally unstable with respect to initiation of erosion and piping at this stage by approximately 8:30 a.m. for conditions corresponding to $k_h \approx 10^{-4}$ cm/s or greater, and hydrostatic forces on the upper clay veneer (overlying the main marsh layer) at the toe region were also marginally unstable with regard to potential hydrostatic uplift for those same conditions. Accordingly, it is possible that initial piping was initiated, but if so it is not likely that it had time to progress much. An important difference between the section at the north breach described earlier, and this south breach, occurs at the inboard side toes of the two sections. The ground surface elevation declines slightly, as one moves progressively north along the landside toes of this overall levee frontage, and there is also a thin fillet of fill at the inboard side of the south breach section. As a result, the relatively impervious cover over the pervious marsh stratum provided by the upper marsh clays was very thin at the north breach (as thin as approximately 3 ft in thickness), whereas the cover provided by the swamp/marsh clays and the fillet of fill over the more pervious marsh stratum at the inboard toe of the south breach section was on the order of 6–8 ft in thickness. Accordingly, potential uplift instability would have developed later in time at this south breach section.

As with the north breach, it was necessary to investigate several competing failure modes at this south breach site.

### Hypothesis No. 1: Potential Underseepage-Induced Lateral Translational Instability

Both limit equilibrium analyses and finite-element analyses were performed to study this, and the results were in excellent agreement; generally within 10% or less of each other at the same water stages and with the same modeling of underseepage-induced pore pressure development at the later stages of the storm surge rise (ILIT 2006).

The conventional limit equilibrium stability analyses were performed using the program SLOPE-W in conjunction with SEEP-W, which was used to perform the necessary transient flow seepage analyses. The coupling of these programs permits the pore pressures (and seepage gradients) from any stage of the time-dependent transient seepage analyses to be imported into SLOPE-W for use in the limit equilibrium stability analyses. In these coupled seepage/limit equilibrium analyses, it was assumed

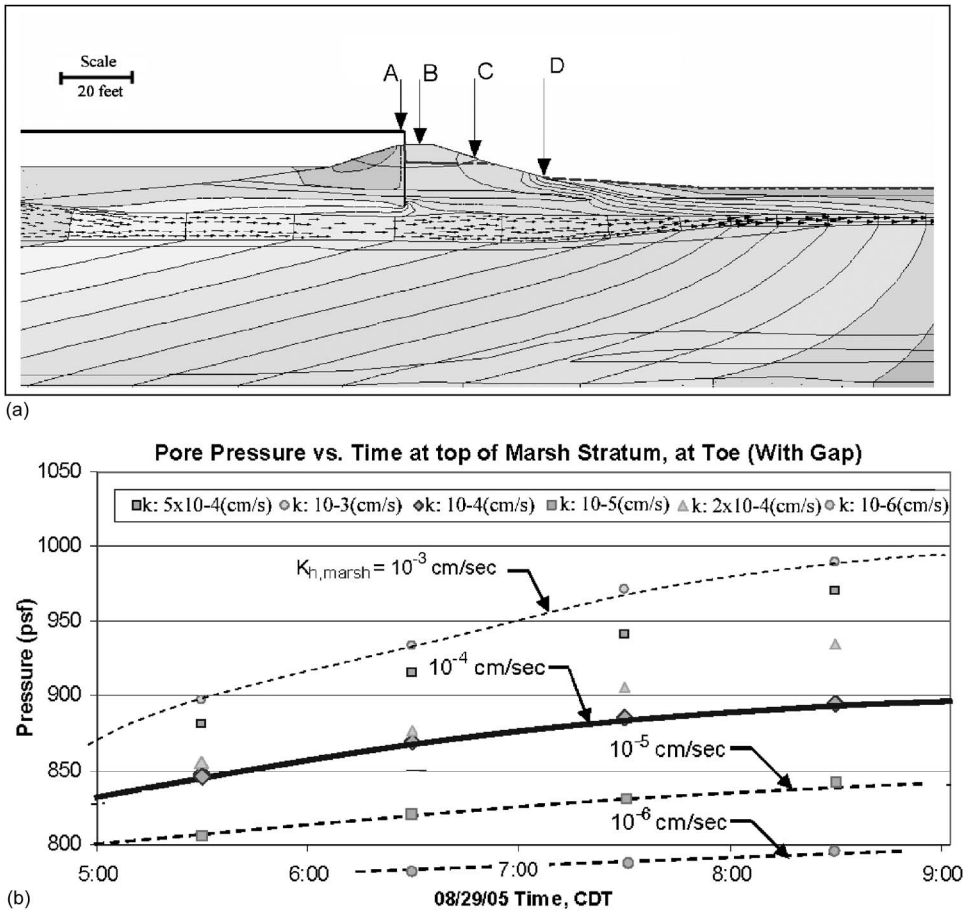


**Fig. 13.** (a) Equipotential contours at the time when canal water levels reached Elev. +14 ft (MSL). Contours are at 1 ft intervals; (b) pore pressure versus time at the top of the marsh stratum directly beneath Location D of Fig. 13(a), as a function of the lateral permeability of the marsh stratum.

that a water-filled gap formed at the outboard side of the sheetpiles/I-wall during the later stages of the storm surge rise, to the full depth of the sheetpile curtain, and lateral water forces were applied against the sheetpile curtain and I-wall over this full depth for the stability analyses.

Similar analyses were performed using the finite-element program PLAXIS (Brinkgreve 2007) to simultaneously model seepage forces, pore pressures, and resulting deformations and displacements. In these finite-element analyses, the shear strength reduction (SSR) method (e.g., Dawson et al. 1999; Griffith and Lane 1999) was used to evaluate the overall factor of safety with respect to lateral translational stability failure at various stages, and for various underseepage/permeability assumptions in the marsh strata.

Fig. 14(a) shows the results of one of the finite-element analyses performed; in this case conforming to conditions at approximately 8:30 a.m., with an IHNC water elevation of +13.5 ft (MSL), and based on underseepage associated with $k_h = 10^{-5}$ cm/s within the main marsh stratum. The shear strain contours in this figure are relative shear strain, which is shear strain developed divided by the shear strain required to result in full shear failure (for a Mohr–Coulomb model). Shear strengths in the foundation soils were again modeled as described in Table 1, except that effective stress parameters were used to model shear strength behavior within the marsh strata so that the effects of underseepage-induced pore pressure increases (which resulted in decreases in shear strengths) could be modeled. These effective stress properties are summarized in Table 1. It was the interaction between underseepage-induced pore pressures and the marsh strata (which were locally capped by less pervious clays) that appears to have led to the strength reduction that may have eventually promoted overall lateral instability of this section.

The progressive formation of a water-filled gap was directly modeled in these incremental finite-element analyses, and Fig. 14(a) has been retouched (for clarity) to show that a partial gap has begun to form (extending to a depth approximately halfway down the combined sheetpile/I-wall, so far) at this stage. The most critical failure surfaces were found by both the finite-element and by the combined seepage/limit equilibrium analyses to be a nearly co-equal pair of mechanisms, as shown in Fig. 14(a). The upper critical potential failure surface was a semirotational mechanism that acted along the top of the thin upper marsh stratum, and the lower potentially critical failure surface was a semirotational failure occurring mainly within the lower (main) marsh stratum, as shown by the lower failure surface in Fig. 14(a).

The lower mode was found to be slightly more critical in the finite-element analyses, and the upper mode was found to be slightly more critical in the coupled seepage/limit equilibrium analyses. The calculated FS for the lower semirotational mode was calculated in the specific analysis shown in Fig. 14(a) to be FS=1.08 (by the SSR method), for conditions when the IHNC water level was at +13.5 ft (just short of its eventual peak at approximately +14.5 ft, MSL), and FS=1.13 was calculated for

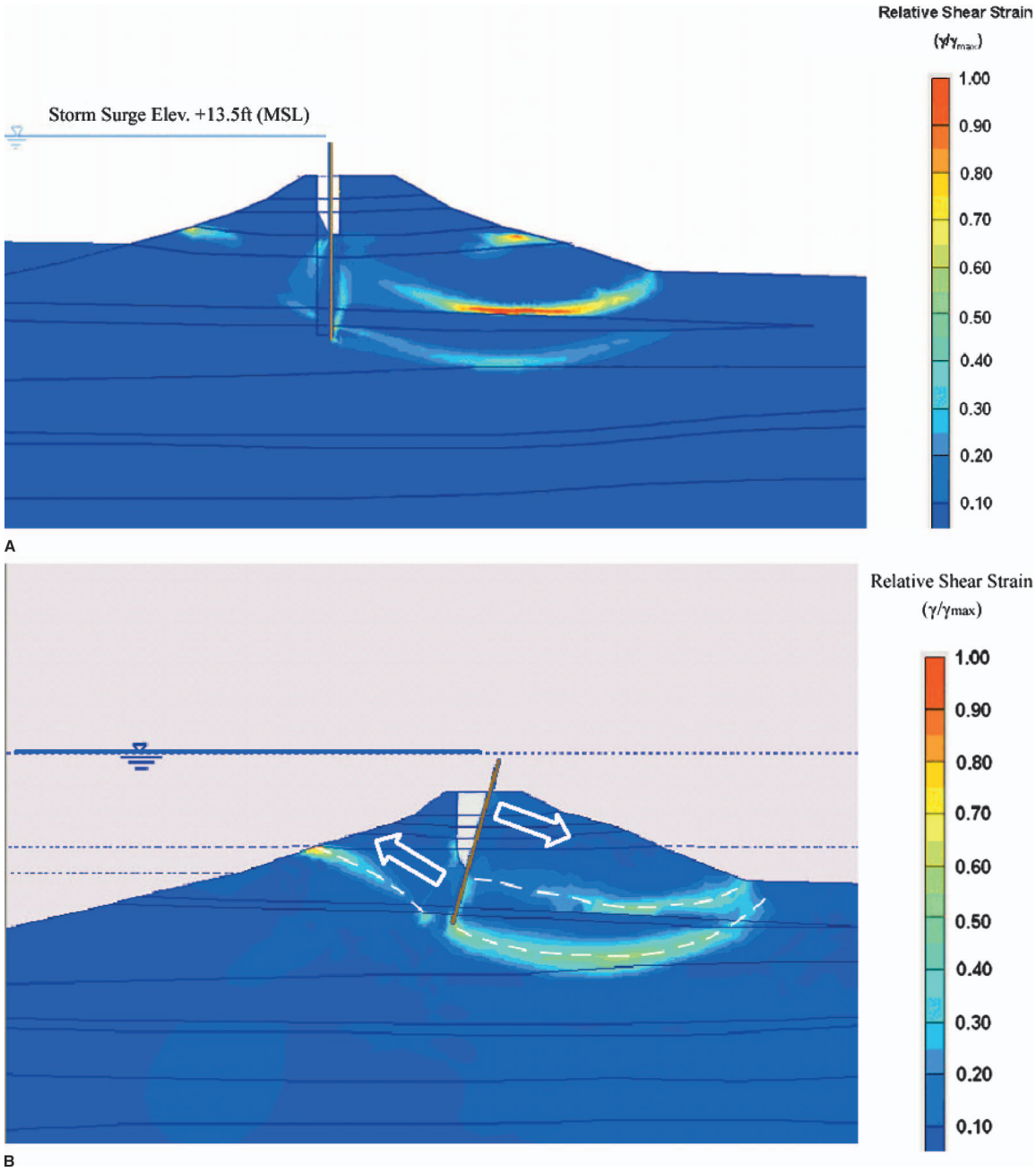


**Fig. 14.** (Color) (a) Finite-element analysis results showing the two most critical potential failure surfaces for the south breach with the IHNC water level at Elev. $\approx +13.5$ ft (MSL), and for pore pressure and underseepage conditions at 8:45 a.m., based on $k_{h,\text{marsh}} \approx 10^{-5}$ cm/s; (b) finite-element analysis results showing stable "cradling" of a partially toppled I-wall and sheetpile curtain, south breach section, IHNC at the west end of the Lower Ninth Ward

the lower mode. It should be noted that the analyses of Fig. 14(a) represent just one canal water elevation, and are based on $k_h = 10^{-5}$ cm/s.

Both the limit equilibrium analyses and the finite-element analyses included the presence of a gap that opened on the outboard side of the sheetpile curtain between the sheetpiles and the outboard section of the levee embankment. This effectively cut the levee embankment in half, and it also admitted water into this gap; significantly increasing the lateral water pressures against the lower portions of the sheetpiles/floodwall and the resisting inboard side of the embankment. As shown in Fig. 15, finite-element analyses showed that this gap likely began to open at canal water levels of approximately +10 to +12 ft (MSL), and opened progressively (to increased depth) thereafter. The analytical details used to model this gap propagation are explained in by Seed et al. (2008c). A third, and also significant, effect of the opening of the gap during the later stages of the storm surge rise was that it allowed pore pressures to be introduced directly at the base of the sheetpile curtain once it opened to full depth.

Fig. 15 shows the calculated evolution of the overall FS for this potential failure mode as a function of progressively rising water levels (over time) in the IHNC, and for two sets of modeled $k_h$ levels within the peaty marsh strata. The results shown are for finite-element analyses, but the results of more conventional seepage/limit equilibrium analyses were similar for the later stages of water rise (generally within 10% or less for most com-

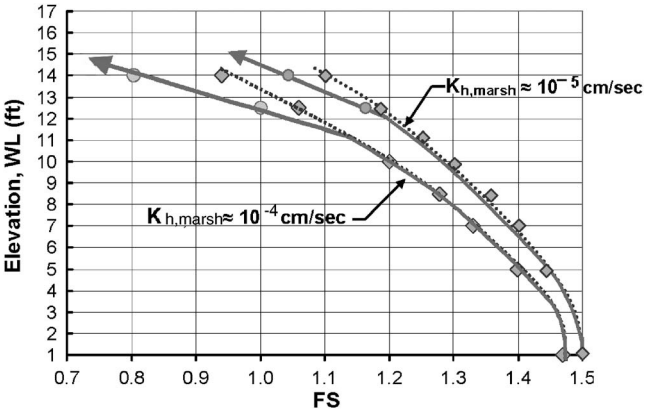


**Fig. 15.** Evolution of factor of safety as IHNC water levels rose; plot of overall factor of safety for lateral translation versus water elevation (south breach on the IHNC, at the west end of the Lower Ninth Ward)

binations of water level and modeled marsh $k_h$). In Fig. 15, the dashed lines and diamond symbols are calculated FS values without the opening of a water-filled gap on the outboard side of the sheetpiles (from analyses where the development of the gap was prevented), and the solid lines (and infilled circles) are the calculated FS values when such gapping is allowed to occur naturally. As shown in this Fig. 15, these finite-element analyses showed that such a gap would begin to open at a canal water level of between +11 and +12.5 ft (MSL). For other ranges of stiffness parameters also considered reasonable, this gap began to open at water elevations of between about +10 to +13 ft (MSL).

Fig. 15 shows results for two assumed sets of lateral hydraulic conductivity conditions within the peaty marsh strata: $k_h = 10^{-4}$ cm/s and $k_h = 10^{-5}$ cm/s. As shown in Fig. 15, these analyses show a reduction to FS $\leq 1$ at water levels of +12.5 and +14.5 ft (MSL), respectively; so that analyses based on lateral marsh permeabilities in this range would largely bracket the observed performance (failure at a canal water elevation of approximately +14 to +14.5 ft, MSL). For lateral marsh permeabilities progressively lower than about $10^{-5}$ cm/s, the calculated values of FS for the full height of water level rise in the IHNC to +14 to +14.5 ft (MSL) progressively begin to rise above 1.0.

### Hypothesis No. 2: Overtopping, Trench Erosion, and Lateral Toppling of the I-Wall

It is also necessary to consider the alternate possibility that overtopping, and resulting erosion of a trench adjacent to the inboard side of the concrete I-wall (as shown previously in Fig. 11), directly served as the primary cause of the failure and breach at this site. Analyses showed that it would be necessary to erode such a trench to a depth of approximately 6.5–8 ft in order to fully topple the I-wall (and its supporting sheetpile wall) laterally under the lateral water pressure loads imposed by a canal water elevation of +14 ft, MSL (ILIT 2006). The erosive trenching observed immediately to the south of the breach site (Fig. 11) was to a depth of typically between 2.5 and 4 ft along most of this frontage, but deepened toward to edge of the breach itself with a maximum observed eroded trench depth of 4.5 ft at the edge of the last portion of intact levee adjacent to the breach itself. That leaves open the question of the likely depth of erosive trenching at the location of the breach itself, as the breached section was catastrophically eroded during the failure and so cannot be examined.

There are no rigorous and well-accepted methods for quantifying the precise rate (and depth) to which such overtopping erosion would occur (Hughes 2006). Accordingly, the approach taken was to examine observed scour produced by overtopping of I-walls at other locations throughout the regional flood protection system during this event. Such erosion of trenches at the inboard sides of overtopped I-walls occurred at numerous locations during hurricane Katrina.

Studying the depths of resulting trench erosion, as a function of water fall height (wall heights above the earthen levee crests), it was observed that the only section that eroded a trench to a depth greater than the water drop height was at the Citrus Back Levee (at Location E, in Fig. 1). Trenching scour occurred to varying depths along this frontage over a distance of more than 1,500 ft, and long sections of the I-wall (and supporting sheetpile curtain) were pushed laterally along this frontage. The deepest trenching measured by our investigation was to a depth of 6.5 ft along this section, slightly more than the approximate 5.5–6 ft water fall height (from the top of the I-wall to the earthen levee crown) at that location. It is suggested that it is unlikely that the approximately 5.5 ft fall height over the I-wall at the south breach at the west end of the Lower Ninth Ward produced a significantly greater eroded trench depth. Finite-element analyses (again with PLAXIS) showed that erosion of a trench to a depth of approximately 6.5–8 ft would be required to topple the I-wall at the maximum water elevation of +14 ft (MSL). That suggests that lateral toppling of the I-wall at the massive south breach was somewhat unlikely, but does not fully rule it out as a possibility.

Analyses of the potential effects of erosion to sufficient depth to laterally topple the unbraced concrete floodwall are thus also of interest. Fig. 14(b) shows finite-element analyses performed for a situation in which overtopping has been assumed to result in erosion of a trench to a depth of 8 ft at the inboard side of the floodwall (sufficient to allow the wall to be pushed sideways by the IHNC water level of +14 ft, MSL), but wherein the underseepage-induced pore pressures (and resulting reduction in foundation soil strengths) are not allowed to cause overall lateral stability failure (as in Hypothesis No. 1, discussed previously). The floodwall in Fig. 14(b) has been laterally displaced (pushed over) by water pressures associated with a canal water level of Elev. +14 ft (MSL), and is now resting against the inboard side of the eroded trench. The configuration, as shown, is stable with a FS (based on the SSR method) of approximately FS = 1.18 with regard to cantilever failure. If lateral embankment failure is precluded, then the most critical failure mode (the one with this FS) is illustrated by the arrow superimposed on the figure; a cantilever failure requiring reverse slippage (with movement to the left in the figure) of the soils laterally supporting the base of the sheetpile curtain. Secondary modes of failure, with higher margins of safety, would include: (1) failure to the right of the upper portion of the levee embankment under the lateral "push" exerted by the upper portion of the I-wall and sheetpile curtain; and (2) a deeper seated, semirotational failure of the overall embankment and floodwall. This analysis thus suggests that simply toppling the I-wall laterally by eroding a trench at its back side, while simultaneously applying water pressures equal to the full surge rise in the IHNC, would not immediately produce a catastrophic failure along the full width of the observed failure.

This is supported by observations of the performance of I-walls at other locations in the region. Fig. 16 shows two examples, at two sections of the Citrus Back Levee (and floodwall) described previously. Fig. 16(a) shows a deeply eroded (scoured) trench on the inboard side of the floodwall, at one of the deepest

(a)

(b)

**Fig. 16.** (a) Significant lateral deflection of the Citrus Back Levee floodwall, seen from the inboard (protected) side. Note the soil heave adjacent to the displaced sheetpiles; (b) deflection and tilting of another section of the Citrus Back Levee floodwall, this time viewed from the outboard side. Note the gap between the outboard side levee embankment and the sheetpile curtain.

scoured sections observed behind these types of walls. The wall leans inboard slightly, and a close look at the sheetpiles at the base of this wall (in the left center of this photograph) shows that this lateral wall deflection resulted in heaving up (or plowing) of soil against the sheetpile curtain at the base of the floodwall, which in turn stabilized the wall in the partially displaced position shown. The lower Fig. 16(b) shows a second long reach of this Citrus Back Levee, this time viewed from the outboard side, where the floodwall (and sheetpile curtain) were pushed laterally to a position cradled by the far side of the eroded trench behind the floodwall [as in Fig. 14(b)]. Again, the wall remained stable in that position until the storm surge had subsided.

This does not mean that the conditions shown in Fig. 14(b) (without significant underseepage) do not represent a potentially feasible failure mechanism. The large lateral displacement of the sheetpiles and I-wall would have resulted in differential movements, and resultant elongation of the sheetpile curtain and I-wall. As noted previously, the sheetpile curtain showed itself to be surprisingly capable of surviving such extensile stresses and deformations while retaining its interlocks, but the concrete I-wall could have broken and spalled off the top (or separation could have occurred between two adjacent concrete panels), and this in turn could have led to uncontrolled erosion (and further propagation of the failure) as floodwaters began to enter through the resulting localized breach in the I-wall and to produce additional scour. The initially localized breach could then have propagated rapidly. Thus, lateral I-wall instability produced by overtopping erosion represents at least a second theoretically feasible candidate mechanism for the failure at this site.

### Hypothesis No. 3: Semirotational Stability Failure through the Top of the Soft Gray Clays

Another potential failure mechanism that requires consideration is a semirotational stability failure through the top of the soft gray clays underlying the marsh strata, as was Hypothesis No. 2 for the north breach. This mechanism proved to have larger associated factors of safety, due largely to the slightly higher ground surface elevation inboard of the levee toe, and so was found not to be a potentially feasible mechanism (FS $\geqslant$ 1.3 at the maximum IHNC water elevation of +14.5 ft, MSL).

### Hypothesis No. 4: Underseepage-Induced Piping and/or Blowout

As discussed previously, analyses performed with different values of $K_h$ consistently showed a higher likelihood of underseepage-induced lateral (semirotational) embankment stability failure than underseepage induced uplift and piping erosion failure. This was due primarily to the slightly greater depth of cover of the peaty marsh stratum at this south breach. In addition, the piping/uplift failure would have been expected to initially produce a narrow failure/breach feature, not the unusually broad (950 ft wide) massive feature that was observed.

**Summary of the Prevailing Failure Mechanism.** In the end, it is our investigation's conclusion that a fully definitive determination cannot be made between the multiple available competing potential failure mechanisms at this site based solely on these conventional geotechnical analyses. The two leading potential candidate mechanisms are: (1) overtopping, producing erosion of a trench on the rear face of the concrete I-wall, and resultant lateral instability of the I-wall; and (2) underseepage-induced reduction of strength in the foundation soils, and resultant lateral stability failure of the inboard half of the levee embankment pushed by lateral water forces exerted against the sheetpile curtain and I-wall. Opinions within our investigation team are somewhat divided, as both mechanisms appear to provide at least potentially feasible explanations

Arguments for the overtopping-induced failure include the clear observation of such erosive scouring of trenches behind overtopped I-walls along this frontage, and the demonstrated feasibility (at least marginal feasibility) of sufficient erosion as to produce lateral wall movement and resultant potential damage to the concrete I-wall. The underseepage-induced failure hypothesis would require either localized lateral hydraulic conductivity of some of the marsh strata along this frontage of $k_h \approx 10^{-4}-10^{-5}$ cm/s, or some additional through-passage of seepage-induced pore pressures through the joints in the sheetpile curtain into the upper marsh stratum.

Some of the most important evidence comes not from geotechnical analyses, which can support the potential feasibility of both mechanisms, but from the field evidence associated with the breach itself. This was a very long breach (nearly 1,000 ft in length), and the evidence suggests that it occurred substantially all at once, as a single cataclysmic event rather than as a progressively widening feature that had initiated at a smaller point of inception. Witnesses described a roar, and then a massive rush of water (Consolidated Litigation 2008), and the homes within the first several hundred feet of the breach, along its full width, were

clearly subjected to massive lateral water forces over essentially the full width of the approximately 950 ft wide feature (see Fig. 9) and were stripped from their foundations and broken up by the inflow. This is not consistent with a localized point of initiation that then propagated (spread) more broadly, as waters would have begun to pond if the initial breach had been a localized feature and the full brunt of the initial inflow would not have been applied along the full breach width.

The overtopping failure hypothesis can be further checked against other overtopping-induced failures (and nonfailures) that occurred during Hurricane Katrina. In addition to the Citrus Back Levee I-wall that was discussed previously (the breach at Location E in Fig. 1), an additional I-wall failure due to overtopping occurred on the west bank of the IHNC, almost directly across the channel (slightly to the north) from the two large breaches at the west end of the Lower Ninth Ward, and this is presented and discussed briefly in a companion paper (Seed et al. 2008b). Here again, the I-wall failure due to overtopping produced a much more localized and noncatastrophic failure; lateral displacement of the I-wall as it became partially unbraced by erosion of a scoured trench at its inboard side resulted in separation of two adjacent concrete I-wall panels, but the damage was very localized and the feature did not then subsequently scour very much and so did not grow into a very large feature.

So it appears that overtopping-induced lateral I-wall instability produced failures of a different character than that observed at the Lower Ninth Ward's south breach. The occurrence of lateral translational embankment stability failure, on the other hand, would well explain the sudden and dramatic failure along a considerable frontage length, and also the resulting apparent sudden lateral force of the unleashed floodwaters along essentially the full length of this large feature.

Finally, it is noted that the $k_h$ of the marsh strata at this site are highly variable. Historic geologic mapping clearly shows the occurrence of northeast trending drainage features passing diagonally across this levee frontage from southwest to northeast, which eventually converge and form the headwaters of Bayou Sauvage just to the east of this failure site (Rogers et al. 2008). There was also a well-established history of underseepage issues along this frontage.

An additional indication of the potential for a zone of pronounced underseepage at the south breach location was provided after the hurricane had passed. Fig. 17 shows a well-developed crevasse splay (the fan-shaped feature in the bottom left corner of the photograph); a classic erosional feature produced by reverse underseepage through the foundation marsh strata at this breach site as the last of the floodwaters drained back into the IHNC from the flooded Lower Ninth Ward beneath the newly completed emergency repair embankment section at the south breach. The gradients that produced this feature would have been very low, as the Lower Ninth Ward had already been largely unwatered by pumping when the repair section was closed, so this classic reverse crevasse splay is an indication of locally problematic soils (with regard to both lateral permeability and erosive potential) underlying the repair embankment at precisely the location of the original failure.

One final piece of evidence is the relatively minor, but noticeable, lateral displacement of a considerable portion of the levee and floodwall along the frontage section between the north and south breaches along this IHNC frontage; as shown in Fig. 18. This photograph shows the I-wall along the frontage between the two major breaches, and is taken from the north breach looking toward the south. The two concrete I-wall panels in the immediate

**Fig. 17.** Reverse crevasse splay produced by reverse drainage out through the foundation soils beneath the interim repair embankment section; south breach IHNC at the Lower Ninth Ward (IPET 2006)

foreground mark the south end of the north breach, and the large barge that passed in through the large south breach can be seen (dimly) in the background; just behind and above truck on the left of the I-wall. As shown in Fig. 18, the I-wall is significantly misaligned between these two major breach features in the wake of Hurricane Katrina. This misalignment did not appear to be associated with significant overtopping-induced trench scour behind the floodwalls; in fact many of the displacements occurred at

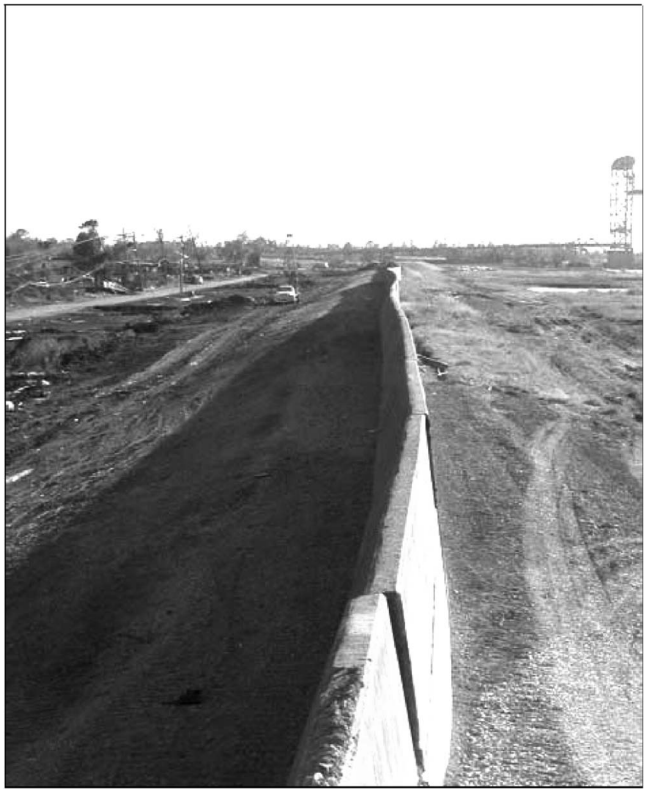

**Fig. 18.** View of lateral misalignment along the I-wall between the north and south breach features; IHNC at the west end of the Lower Ninth Ward (IPET 2007)

locations that exhibited little or no scour of that sort. Instead, the misalignment appears to have been due to deeper-seated movements; movements that could apparently only be explained as partial or incipient lateral translational displacement of the levee embankment itself.

In the end, it is the conclusion of our (ILIT) studies that the preponderance of the evidence appears to favor underseepage-induced lateral translational failure as the most likely cause of the failure and breach at this site, but that the alternate hypothesis of overtopping-induced failure is also plausible and cannot be fully discounted.

## Conclusion

The devastating damages produced by the flooding of New Orleans during Hurricane Katrina resulted in substantial human and financial losses. Numerous breaches along the GIWW/MRGO and IHNC channels resulted from several sets of causes. One common cause was the occurrence of failures at "transitions" between two separate sections of the flood protection system. This was a repeated theme throughout the overall region, and it serves to point out:

1. The importance and difficulty of designing and constructing compatible transitions (or connections), and the need to give them extra attention.
2. The difficulties intrinsic in construction of large regional flood protection systems over periods of multiple decades as a result of current governmental approval and appropriations processes. These systems must function well as *systems*, with all of the individual elements meshing together seamlessly in a mutually supportive manner. Construction of these systems "in bits and pieces," and over long periods of time, during which personnel changes can result in loss of continuity and institutional memory, is not ideal.
3. A significant number of failures occurred at penetrations where utilities and/or other infrastructure pass through the levee frontages. These represent locations where multiple overlapping agencies and interests, and overlapping jurisdictions, can render it difficult to ensure a safe transition between project elements. In the future, public safety should come first ahead of other competing interests. In addition, a single agency should be in overall charge at such penetrations, and they must have adequate authority as to be able to impose a safe overall solution if conflicts arise.

A third set of failures, and partial failures, in this central region were due to overtopping and erosion, often at transitional contacts between structural elements and earthen embankment sections. The overtopping was exacerbated by the fact that the USACE had progressively lost track of its elevation control over the several decades of construction of the levees and floodwalls due to ongoing settlement of regional benchmarks, which resulted in many of the levees and floodwalls having crest elevations between 1 and 2 ft below their original Congressionally authorized design grade (IPET 2007; Wooley and Shabman 2007). Additional erosional features can also be attributed to the use of highly erodeable soils, including both cohesionless sands and also lightweight shell sands, as levee embankment fills at some locations; three such locations occurred on the west bank of the IHNC near the south end, and these will be discussed further in a companion paper (Seed et al. 2008b). Two additional locations with highly erodeable shell sand fills were noted on the east bank of the IHNC, at the west end of the New Orleans East protected basin. At these locations, highly erodeable shell sand mixes (which pose an intrinsic hazard with regard to their unusually high erosion potential) were present without internal cut-offs to prevent through-flow seepage and erosion, and without crest and face protection to prevent erosion due to wave attack or overtopping. It is unlikely that all such locations containing highly erodeable shell sand fill along the IHNC were daylighted during Hurricane Katrina, and one of our recommendations is that further studies be undertaken to look for additional sites where such materials may be present (especially near to transitions and penetrations) along the banks of the IHNC. If such sites are found, they need to be addressed.

Finally, significant effort was devoted to determination of the causes of the two large failures on the east bank of the IHNC, at the west end of the Lower Ninth Ward. At each of these two important breach locations, multiple modes represented at least potentially feasible explanations for the failures observed, making final determination of the precise cause(s) of these two major failures challenging.

The most likely cause of the north breach was underseepage-induced erosion and piping, initially exacerbated by underseepage-induced hydraulic uplift near the inboard toe. A critical issue here is the likely lateral hydraulic conductivity of the peaty marsh stratum in the upper foundation soils. Our conclusions are based in part on our interpretation of the ability of this layered and variable stratum to transmit pore pressures from the storm surge laterally beneath the levee and floodwall (and short sheetpile curtain), and are supported by our seepage and stability analyses, and also by the observed timing and geometry of this failure. While the alternate mechanism of lateral, semirotational stability failure cannot be fully discounted, it appears to be less likely based on the observed postfailure field geometry and available geotechnical data.

Similarly, underseepage-induced reduction in foundation soil strengths, and consequent lateral translational stability failure of the levee embankment and floodwall, was the most likely cause of the massive south breach. A second possibility would be that overtopping erosion and resultant scouring of an eroded trench behind the floodwall resulted in laterally unbracing of the floodwall, and that elevated IHNC canal water levels then pushed the floodwall sideways producing the failure. Although it appears the less likely of the two potential failure modes, this second hypothesis that cannot be fully discounted. Important arguments for the underseepage-induced lateral stability failure include: (1) the unusual length (950 ft) of the failure; (2) the massive lateral water forces exerted against the inboard side community along the full width of the breach (suggesting sudden onset, rather than propagating from a localized initiation point); (3) a history of underseepage along this levee frontage; and (4) lateral displacements of adjacent I-wall sections that also appear to be deep-seated features that are not associated with overtopping and trench scour behind the floodwalls.

There were multiple competing potential failure mechanisms operating simultaneously at both of these major breach sites. The suites of potential mechanisms associated with underseepage were not considered in the original design analyses as it was assumed that the foundation soils were insufficiently pervious as to transmit large underseepage-induced pore pressures beneath the (shallowly embedded) floodwalls during the relatively short duration of a hurricane-induced storm surge (USACE 1966). This highlights the importance of considering all potential failure modes during design, and also during postfailure forensic investigations.

It appears that the two major, and catastrophic breaches at the west end of the Lower Ninth Ward might both have been prevented if the shallow sheetpile curtains (which were less than 20 ft in depth at both sites) had been extended 8–12 ft deeper; fully "cutting off" underseepage flow through the marsh strata at those depths and achieving secure hydraulic tie-in (embedment) within underlying, relatively impervious clays. Extending these to greater depth would also have likely eliminated the potential cantilever failure due to scouring of a trench behind the wall at the south breach, and would also have served to increase the lateral stability of both embankment sections by driving any potential translational or rotational failure surfaces deeper.

This was a costly lesson, and one to be seriously considered in other parts of the nation where optimistic assessments regarding likely hydraulic conductivity and seepage behaviors of both levees and their foundation soils are not sufficiently uncommon. A more defensive, conservative approach with regard to soils whose hydraulic conductivity is difficult to assess would appear to be warranted.

## Acknowledgments

The studies reported herein would not have been possible without the generous help of many individuals and organizations. A more detailed and extensive acknowledgment is presented in the first of the companion papers and for the sake of brevity is not repeated here. This project was supported, in large part, by the National Science Foundation (NSF) under Grant Nos. CMS-0413327 and CMS-0611632. Any opinions, findings, and conclusions or recommendations expressed in this material are those of the writers and do not necessarily reflect the views of the NSF. Additional support was provided by the Center for Information Technology Research in the Service of Society (CITRIS) at the University of California at Berkeley. In addition, several senior members of the investigation team contributed from their own discretionary resources. All of this support is gratefully acknowledged.

## References

Bear, J. (1972). *Dynamics of fluids in porous media*, Dover, London.

Beckwith, C. W., Baird, A. J., and Heathwaite, A. L. (2002). "Anistropy and depth-related heterogeneity of hydraulic conductivity in a bog peat. I: Laboratory measurements." *Hydrological processes*, Vol. 17, Wiley, London, 89–101.

Beckwith, C. W., Baird, A. J., and Heathwaite, A. L. (2003). "Anisotropy and depth-related heterogeneity of hydraulic conductivity in a bog peat. II: Modeling the effects on groundwater flow." *Hydrological processes*, Vol. 17, Wiley, London, 103–113.

Bell, F. G. (2000). "Chapter 7: Organic soils: Peat." *Engineering properties of soils and rocks*, Blackwell Science Ltd., Oxford, U.K., 202–476.

Brinkgreve, R. (2007). "*PLAXIS* 2D. Version 8.5 finite-element code for soil and rock analyses." *Complete set of manuals*, R. Brinkgreve ed., Balkema, Rotterdam, Brookfield.

Consolidated Litigation. (2008). Katrina Canal Breaches, United States District Court, Eastern District of Louisiana.

Dawson, E. M., Roth, W. H., and Drescher, A. (1999). "Slope stability analysis by strength reduction." *Geotechnique*, 49(6), 835–840.

External Review Panel (ERP). (2007). "The New Orleans hurricane protection system: What went wrong and why." *ASCE Rep.*, ⟨http://www.asce.org/files/pdf/ERPreport.pdf⟩ (June 4).

Griffiths, D. V., and Lane, P. A. (1999). "Slope stability analysis by finite-elements." *Geotechnique*, 49(3), 387–403.

Hogan, J. M., van der, Kamp G., Barbour, S. L., and Schmidt, R. (2006). "Field methods for measuring hydraulic properties of peat deposits." *Hydrological processes*, Vol. 20, Wiley InterScience, London, 3635–3649.

Hughes, S. A. (2006). "Protection for backside levee slopes." *Draft Rep. to the New Orleans District, U.S. Army Corps of Engineers*, Washington, D.C.

Independent Level Investigation Team (LILIT). (2006). "Investigation of the performance of the New Orleans regional flood protection systems during Hurricane Katrina." *Final Rep.*, ⟨http://www.ce.berkeley.edu/~new_orleans/⟩ (July 31, 2006; Rev. Sept. 10, 2006).

Interagency Performance Evaluation Task Force (IPET). (2006). "Performance evaluation of the New Orleans and Southwest Louisiana hurricane protection system." *Draft Final Rep. of the Interagency Performance Evaluation Task Force*, ⟨https://ipet.wes.army.mil/⟩ (June 1, 2006).

Interagency Performance Evaluation Task Force (IPET). (2007). "Performance evaluation of the New Orleans and Southwest Louisiana hurricane protection system." *Final Rep. of the Interagency Performance Evaluation Task Force*, ⟨https://ipet.wes.army.mil/⟩ (November 2007).

Krahn, J. (2004). "GeoStudio 2004." *Complete set of manuals*, J. Krahn, ed., Calgary, Alba., Canada.

Ladd, C. C., and DeGroot, D. (2003). "Recommended practice for soft ground site characterization." Arthur Casagrande Lecture, *12th Panamerican Conf. on Soil Mechanics and Geotechnical Engineering*, Boston.

Ladd, C. C., and Foott, R. (1974). "A new design procedure for stability of soft clays." *J. Geotech. Engrg. Div.*, 100(GT7), 763–786.

Mesri, G., and Ajlouni, M. (2007). "Engineering properties of fibrous peats." *Commun. Anal. Geom.*, 133(7), 850–866.

Rogers, J. D., Boutwell, G. P., Schmitz, D. W., Karadeniz, D., Watkins, C. M., Athanasopoulos-Zekkos, A., and Cobos-Roa, D. (2008). "Geologic conditions underlying the 2005 17th Street canal levee failure in New Orleans." *J. Geotech. Geoenviron. Eng.*, 134(5), 583–601.

Seed, R. B., Bea, R. G., Abdelmalak, R. I., Athanasopoulos-Zekkos, A., Boutwell, G. P., Briaud, J-L., Cheung, C., Cobos-Roa, D., Ehrensing, L., Govindasamy, A. V., Harder, L. F., Inkabi, K. S., Nicks, J., Pestana, J. M., Porter, J., Rhee, K., Riemer, M. F., Rogers, J. D., Storesund, R., Vera-Grunauer, X., and Wartman, J. E. (2008a). "New Orleans and Hurricane Katrina. I: Introduction, overview, and the East Flank." *J. Geotech. Geoenviron. Eng.*, 134(5), 701–739.

Seed, R. B., Bea, R. G., Athanasopoulos-Zekkos, A., Boutwell, G. P., Bray, J. D., Cheung, C., Cobos-Roa, D., Cohen-Waeber, J., Collins, B. D., Harder, L. F., Kayen, R. E., Moss, R. E. S., Pestana, J. M., Porter, J., Riemer, M. F., Rogers, J. D., Storesund, R., Vera-Grunauer, X., and Wartman, J. E. (2008b) "New Orleans and Hurricane Katrina. IV: The Orleans East Bank (metro) protected basin." *J. Geotech. Geoenviron. Eng.*, 134(5), 762–779.

Seed, R. B., Bea, R. G., Athanasopoulos-Zekkos, A., Boutwell, G. P., Bray, J. D., Cheung, C., Cobos-Roa, D., Harder, L. F., Moss, R. E. S., Pestana, J. M., Porter, J., Riemer, M. F., Rogers, J. D., Storesund, R., Vera-Grunauer, X., and Wartman, J. E. (2008c). "New Orleans and Hurricane Katrina. III: The 17th Street canal." *J. Geotech. Geoenviron. Eng.*, 134(5), 740–761.

Shepard, R. G. (1989). "Correlations of permeability and grain-size." *Ground Water*, 27(5), 633–638.

Spencer, E. (1967). "A method of analysis of the stability of embankments assuming parallel interslice forces." *Geotechnique*, 17(1), 11–26.

URS Corporation/Jack R. Benjamin & Associates, Inc. (2007). "Topical area, levee vulnerability, draft 2." *Technical Memorandum*, Delta Risk Management Strategy (DRMS) Phase 1, Prepared for Dept. of Water Resources, Sacramento, Calif.

U.S. Army Corps of Engineers (USACE). (1966). "General design, Lake

Pontchartrain, LA and vicinity, Chalmette area plan." *Design Memorandum No. 3*, U.S. Army Engineer District, New Orleans.

Van Heerden, I. L., Kemp, G. P., Mashriqui, H., Sharma, R., Prochaska, B., Capozzoli, L., Theis, A., Binselam, A., Streva, K., and Boyd, E. (2006), "The failure of the New Orleans levee system during Hurricane Katrina." *State Project No. 704-92-0022, 20*, ⟨http://www.publichealth.hurricane.lsu.edu/TeamLA.htm⟩.

Wooley, D., and Shabman, L. (2007). "Decision making chronology for the Lake Pontchartrain & vicinity hurricane protection project." *Draft Final Rep. for the Headquarters, USACE*, ⟨http://www.iwr.usace.army.mil/inside/products/pub/hpdc/DraftFinalHPDC3.pdf⟩.

Wright, S. G. (1999). "UTEXAS4—A computer program for slope stability calculations." Shinoak Software, Austin, Tex.